CORAL AND SPELEOTHEM *IN SITU* MONITORING AND GEOCHEMICAL ANALYSIS: GUAM, MARIANA ISLANDS, USA

By

Tomoko Bell
John W. Jenson
Mark A. Lander
Richard H. Randall
Judson W. Partin
Benjamin Hardt
Jay L. Banner

WERI
WATER AND ENVIRONMENTAL RESEARCH INSTITUTE OF THE WESTERN PACIFIC
UNIVERSITY OF GUAM

Technical Report No. 136

December 2011

CORAL AND SPELEOTHEM *IN SITU* MONITORING AND GEOCHEMICAL ANALYSIS: GUAM, MARIANA ISLANDS, USA

By

Tomoko Bell[1]
John W. Jenson[1]
Mark A. Lander[1]
Richard H. Randall[1]
Judson W. Partin[2]
Benjamin Hardt[2]
Jay L. Banner[2]

[1] Water and Environmental Research Institute of the Western Pacific,
University of Guam UOG Station, Mangilao, Guam 96923

[2] Jackson School of Geosciences, University of Texas, Austin,
Austin, Texas, 78751

Technical Report No. 136

December 2011

The activities on which this report is based were financed in part by the Department of the Interior, U.S. Geological Survey, Guam Hydrologic Survey and Pacific ENSO Application Center, through the University of Guam Water and Environmental Research Institute of the Western Pacific. The content of this report does not necessarily reflect the views and policies of the Department of the Interior, nor does the mention of trade names or commercial products constitute their endorsement by the United States Government.

ABSTRACT

The purpose of this study was to initiate reliable, correlative, modern and ancient baseline proxy data for Guam's past hydrologic and climatic conditions using geochemical records accumulated in live coral from its coastal water and in speleothems from coastal caves. Two coastal marine sites were studied: (1) Gabgab Beach, which is well inside Guam's Apra Harbor on the west-central coast; and (2) Haputo Bay, which is 25 km to the northeast on the northwest coast, and faces the open ocean across a platform reef. Coral cores were extracted at each site. Cores were drilled with a novel instrument designed especially for the project; details of the design and application are reported herein. Also included in the study was dripwater from Jinapsan Cave, on the north coast, which is being collected as part of a complementary study of the speleothem record on Guam. Monthly measurements of sea surface temperature (SST), seawater $\delta^{18}O$, and seawater Sr/Ca were taken at one or both of the Gabgab and Haputo sites. We also monitored $\delta^{18}O$ rainwater collected on the University of Guam (UOG) campus on the east-central coast, and $\delta^{18}O$ cave dripwater from Jinapsan Cave. In addition, we monitored nitrate at the Gabgab site and drip water from two sites in Jinapsan Cave to investigate the biological influence on the calcification of coral and speleothems. An *amount effect* for $\delta^{18}O$ was observed in local precipitation. Monthly seawater samples at the Gabgab site showed seasonal variations in SST, $\delta^{18}O$ and nitrate. SST at the Gabgab and Haputo sites were strongly correlated. Both sites also showed strong correlation with the regional SST record. $\delta^{18}O$ measured at the Gabgab site was also correlated with the SST record and local station rainwater $\delta^{18}O$. The concentrations of nitrate at the Gabgab site do not appear to have had any significant affect on the coral calcification system.

The Gabgab coral core revealed interesting correlations between the Sr/Ca signal and wet-dry climatic conditions on Guam. (The Haputo core proved unsuitable for analysis). The Gabgab core contained some 60 annual bands. Sr/Ca and Hadley SST signals from 1960 to 2010 show the same long-term trends. Sr/Ca shows a relatively strong relationship with maximum air temperature, but not with sea level, ENSO index, or precipitation. Sr/Ca from December to March, dry season segment, showed much higher correlation with Hadley SST than the wet season segment (June to September). It is thus inferred that some factors related to wet season influence the relationship between SST and coral Sr/Ca.

KEYWORDS: Guam, Climate Reconstruction, Climate Proxy, Coral Core, SST, Sr/Ca, Speleothem, $\delta^{18}O$, Seawater, Rainwater, Dripwater, Precipitation, Underwater Drill.

ACKNOWLEDGEMENTS

I am very thankful to have an incredibly supportive family, Ryan and Heagen. Thank you for being patient and cooperative for my project for the past two years and helping me sample at the beaches. You two mean everything to me. I thank Dr. Jenson for hiring and sending me to school, agreeing to conduct and coordinate this expensive project and patiently proofreading manuscripts. Thank you to Dr. Denton for financial support, good beer, and conversation. Thank you for Dr. Lander's financial support, great and sharp advice for climatology. I appreciate Professor Randall being on my thesis committee and providing me great insights, especially biological advice. I am fortunate to have the best committee members in this environmental science program. I appreciate Dr. Partin for showing me the fascinations of geochemistry and helping me set up the experimental protocol for coral monitoring and analysis, MatLab training, and much more. Without talking with you in January, 2009, I would not be doing what I am doing now. I truly appreciate the hard work and continuous help from Mr. Tetsuya Endo for making the best underwater drill for this project and taking care of my anxieties over the challenge. Thank you very much to the dive safety officer, Mr. Jason Miller, for coral core sampling at Gabgab Beach and Haputo Bays. Without you, I would be drilling all day long. Thank you to Mr. Chip Guard for kind words and support. I am fortunate to have strong supports from the University of Texas, Austin. Thank you to Dr. Quinn, Dr. Taylor, Dr. Banner, Dr. Hardt, Ms. Meaghan Gorman, Mr. Chris Maupin, Ms. Kelly Hereid and Mr. Kaustaubh Thirumalai. Working at Dr. Quinn's lab for two weeks was one of the best and most fantastic experiences in my life. Thanks to Dr. Quinn for accepting my visit for two weeks and for generously providing the use of his laboratory, and for his advice and support of the analyses. Thank you to Dr. Taylor for taking X-rays and valuable advice for underwater drilling, Mr. Maupin for helping me prepare the coral slabs, Ms. Gorman for patiently and greatly assisting me with Micro-Mill, running the machine for coral samples and creating dataset. Thanks to Ms. Hereid and Mr. Thirumalai for assisting me and Dr. Hardt for meticulous metal analysis. I couldn't complete this project without assistance from my awesome coworkers who keep motivating and comforting me, Mr. John Jocson, Mr. Nate Habana, Mr. Blaz Miklavic, Ms. Maria Kottermair, Ms. Vivianna Bendixon, Ms. Christine Simard and Mr. Van Ayutthaya. I especially thank to Mr. Jocson for training me in Jinapsan Cave, Mr. Habana for providing me the best advice ever, Mr. Miklavic for being my best caving buddy, Ms. Kottermair for keeping me straight and feeding good drinks. Ms. Bendixon, Ms. Simard and Mr. Ayutthaya are my light at WERI office. I also thank to Ms. Jennifer Cruz for laboratory assistance and training, and Ms. Norma Blas and Ms. Gwen Manglona for their kind support. Lastly, I am thankful for my old pals from the Hokkaido University, Dr. Kuroda, Dr. Tsuboi and Dr. Iida for the support and continuous inspiration. You guys are proving to me that our school sprit thrives anywhere in the world. This project was funded by United Geological Survey (grant number: 11HQPA 30002), Guam Hydrological Survey, Pacific ENSO Application Center (grant number: 65A283), WERI and MARC at the University of Guam. I thank to Guam Department of Agriculture for issuing the permit for coral sampling and US Navy for the boat access to Gabgab Beach.

Tomoko Bell

TABLE OF CONTENTS

LIST OF TABLES

LIST OF FIGURES

EXECUTIVE SUMMARY

Purpose and Significance of Study

The purpose of this study was to initiate reliable, correlative, modern and ancient baseline proxy data for Guam's past hydrologic and climatic conditions using geochemical records accumulated in live coral from its coastal waters and in speleothems from coastal caves. Knowledge of local pre-historic hydrologic conditions is of high value for long-term planning and management of Guam's surface and groundwater resources. Reliable historical climatic data from Guam is uniquely valuable to regional and global climate studies because the island is strategically positioned on the northeastern margin of the West Pacific Warm Pool, where it experiences strong ENSO effects, strong seasonality in precipitation (with March-April the driest and August-September the wettest months, with 70% of precipitation from July-December), and occasional heavy tropical storms (typically associated with El Niño events). Moreover, the island is sufficiently small and distant from continental influence to record unperturbed regional marine climatic conditions. The fortuitous co-location of readily accessible corals and speleothems with local research facilities makes Guam exceptionally well-suited for long-term studies of modern conditions and processes in this important tropical zone. To our knowledge, this is the first paleoclimatic study of co-located coral and speleothem records.

Primary Study Sites

Two coastal marine sites were studied: (1) Gabgab Beach, which is well inside Guam's Apra Harbor on the west-central coast; and (2) Haputo Bay, which is 25 km to the northeast on the northwest coast, and faces the open ocean across a platform reef. Coral cores were extracted at each site during the summer of 2009. Cores were drilled with a novel instrument designed especially for the project; details of the design and application are reported herein and by Bell et al., 2011. The Gabgab sampling site, which is on the reef platform in 1-2 m of water, 90 m from the beach and just a few meters off the end of an artificial jetty, was the most comprehensively and consistently monitored. At the Haputo site, the coral core was extracted in the open ocean just outside the reef, while seawater samples were subsequently taken in the bay, on the other side of the reef, in a few meters of water, and 10 m from the shore. Also included in the study was dripwater from Jinapsan Cave, on the north coast, which is being collected as part of a complementary study of the speleothem record on Guam.

Water Chemistry Sampling Program

Monthly measurements of sea surface temperature (SST), seawater $\delta^{18}O$, and seawater Sr/Ca have been taken at one or both of the Gabgab and Haputo sites (August 2009 to present). We also monitored rainwater $\delta^{18}O$ collected on the University of Guam (UOG) campus on the east-central coast (October 2008 to present), and cave dripwater $\delta^{18}O$ from Jinapsan Cave (June 2008 to present). In addition, we monitored nitrate at the Gabgab site (September 2009-September 2010) and dripwater from two sites in Jinapsan Cave (July 2010-November 2010) to investigate the biological influence on the calcification of coral and speleothems.

1. <u>Rainwater $\delta^{18}O$</u>
   To test the presumed *amount effect* in local precipitation, we compared precipitation (October 2008-August 2009) from eight sites across the island to rainwater $\delta^{18}O$ measured at UOG. Six site showed strong correlation ($r < -0.79$) and two showed more modest correlation ($-0.6 < r < 0$).

2. <u>Gabgab and Haputo Seawater SST and $\delta^{18}O$</u>
   Monthly seawater samples at the Gabgab site showed seasonal variations in SST, $\delta^{18}O$ and nitrate. Concurrently measured SST (September 2009-January 2010) at the Gabgab site and the Haputo site were strongly correlated ($r = 0.98$). Notably, both sites also showed strong correlation with the regional Hadley SST record (Gabgab-Hadley, $r = 0.93$; Haputo-Hadley, $r = 0.98$). Mean seawater $\delta^{18}O$ at the Gabgab site (September 2009-October 2010) was -0.52‰ with extremes of -0.3‰ in February and -0.7‰ in September. Gabgab $\delta^{18}O$ was also correlated with the Hadley SST record ($r = -0.88$) and local (UOG station) rainwater $\delta^{18}O$ ($r = 0.90$).

3. <u>Gabgab Nitrate</u>
   Nitrate concentration at the Gabgab site dropped from a high of ~0.06 mg/L in October 2009 to below detection limit (BDL) in February 2010, where it remained through the end of the sampling period in September 2010. From September to March, nitrate was strongly correlated with precipitation measured at a nearby station, decreasing in line with the general decline in precipitation, until reaching BDL in February. There was also a strong correlation with the Hadley SST record ($r = 0.90$) from October 2009 to March 2010. The concentrations of nitrate at Gabgab do not appear to have had any significant affect on the coral calcification system.

4. <u>Jinapsan Cave Nitrate and Alkalinity</u>
   At Jinapsan Cave, the mix of rainwater water collected from August to October 2010 showed ~0.02 mg/L of nitrate. Dripwater collected at the two fastest-dripping stations (the only ones that yielded enough surplus water to support the additional analysis for nitrate) from July to November 2010 showed much higher concentrations of 3.20 and 1.92 mg/L. Alkalinities measured at these same two stations showed constant trends from February 2009 to June 2010, with alkalinity consistently higher at one of them. There was no significant correlation between alkalinity level and precipitation.

<u>Coral Sr/Ca Signal Interpretations</u>

Seawater samples were collected at both sites to test whether the widely employed assumption of conservative seawater chemistry is valid in the coastal waters of Guam (for Sr and Ca, in this case), particular for the Gabgab site, which lies inside a harbor, in shallow water close to the shore; laboratory analysis of the seawater Sr/Ca samples from each site is still underway. In the meantime, the Gabgab core has revealed interesting correlations between the Sr/Ca signal and wet-dry climatic conditions on Guam. (The Haputo core proved unsuitable for analysis). The Gabgab core contained some 60 annual bands, within each of which the sampled point with the highest Sr/Ca values was assigned to February.

1. Sr/Ca vs. SST
   Coral Sr/Ca and Hadley SST signals from 1960 to 2010 show the similar long-term and intermediate trends. Sr/Ca from December to March (dry season/short daylight/lower SST segment) showed much higher correlation with Hadley SST than June to September (wet season/long daylight/higher SST segment).

2. Sr/Ca vs. Air Temperature, Sea Level, ENSO Index and Precipitation
   In addition to the comparison to SST, we compared 12-month averages of Sr/Ca against maximum air temperature (Andersen AFB record), local sea level, the ENSO index and precipitation (Andersen AFB record). Coral Sr/Ca and maximum air temperature show a relatively strong relationship, while sea level, the ENSO index and precipitation, on the other hand, do not show strong relationships.

1.0 Preface

The results reported here are from geochemical research to establish a reliable baseline for climate proxy studies of the hydrologic history of Guam, Mariana Islands, USA. Guam is located in the eastern sector of the Western Pacific Warm Pool (WPWP). It is well known that the WPWP plays a key role in the earth's climate system, with strong links to El Niño and La Niña. Global climate history has been receiving great attention worldwide, and some WPWP geochemical climate studies using corals or speleothems have already been conducted (cf., Asami et al., 2005, Quinn et al., 2006, Partin et al., 2007). However, previous studies in the tropics lack regular, long term *in situ* monitoring, which will aid sea surface temperature (SST) and precipitation to be reconstructed more accurately, and help us better understand the coral and speleothem geochemical records. This is due to the simple fact that all the studied corals and speleothems to date are remote from academic facilities; therefore, regular *in situ* monitoring has been infeasible.

Since $\delta^{18}O$ and Sr/Ca are widely used chemical species in paleoclimatology, we conducted monthly monitoring of SST, $\delta^{18}O$ in seawater, Sr/Ca in seawater, $\delta^{18}O$ in rainwater and $\delta^{18}O$ in cave dripwater at selected coral and speleothem sites on Guam. To our knowledge, this is the first continuous *in situ* monitoring of coral and cave sites in the tropics. Using this dataset and analyzing a 60-year-old coral geochemically, we also evaluated past SST in Apra Harbor on Guam. In addition, we analyzed nitrate in seawater and dripwater to investigate the biological influence on the calcification system of coral and speleothems.

There are at least seven types of proxies commonly used to investigate past climate using geochemical and related clues: (1) ocean or lake sediments (2) ice cores (3) speleothems (4) tree rings (5) corals (6) planktonic foraminifera, and (7) pollens. However, past studies have shown that different proxies can produce disparate results, which can be difficult to reconcile. Even the pioneering 1981 Climate Long Investigation Mapping and Prediction (CLIMAP) study left many unresolved questions in regard to SST in the tropical regions (Crowley, 2000). To resolve such uncertainties, scientists have relied more heavily on using different types of proxies in combination to evaluate the climate history of a given region. For example, Betancourt et al. (2002) compared the results from speleothems and tree rings in New Mexico, USA to study precipitation history for the past 10,000 years. McDermott et al. (2001) measured the oxygen isotope records in speleothems and ice cores to analyze the temperature for the past 10,000 years. Charles et al. (1996) used both deep ocean sediment cores and ice cores to reconstruct ocean current change for 80,000 years. Cook (1995) chose tree rings and corals to study the temperature history on a global scale for the past 100 years. Neukom et al. (2010) combined tree rings, lake and marine sediments, ice cores and corals to reconstruct surface air temperature. Furthermore, Li et al. (2010) noted that some proxies are good for short time scale while others are more appropriate for long term scale analysis, so combining the different proxies takes advantage of complementarities among available proxies.

For this research project, we have combined coral and speleothem data to study past climate history for the region around Guam. This is the first study to consolidate coral and speleothem data from one locale. We believe this multi-proxy study will make climate reconstructions more robust. Moreover, this multi-proxy approach, combined with *in situ* monitoring will have a greater degree of reliability in investigating regional dynamic phenomena such as El Niño, which is of obvious significance not only locally but throughout the world.

2.0 *In situ* water chemistry monitoring for corals and speleothems

2.1 Introduction

In spite of its advantages, the multi-proxy approach relies on certain assumptions that warrant acknowledgement. For example, SST reconstructions using coral $\delta^{18}O$ and Sr/Ca rely on two assumptions in almost all studies: (1) the population and activity of symbiotic algae, zoo-xanthellae, in corals do not affect the uptake of $\delta^{18}O$ and Sr/Ca, and (2) the ratio of $\delta^{18}O$ and Sr/Ca in seawater are very stable through the year for the coral calcification system (i.e., exhibit negligible anomaly. Cohen et al. (2002) argued for the validity of the first assumption, stating that coral Sr/Ca is dominated by photosynthesis level instead of SST. Coral skeleton aragonite is precipitated through a biological process that is not well understood, and none of the geochemical studies to date have critically examined this assumption. Correge (2006) summarized the literatures that investigated SST and Sr/Ca relationships; a few of the coral samples indeed showed no correlation, while most of them displayed high correlation. Thus, he emphasized the significance of looking for biological factors that might affect Sr/Ca in corals. Regarding the second assumption, even though it is a straightforward process to test these chemical species ($\delta^{18}O$, Sr and Ca) in seawater, few studies have rigorously examined this assumption because most of the academic facilities are distant from sample sites. To our knowledge, there is only one other study to date which conducted *in situ* $\delta^{18}O$ in seawater monitoring around corals (Al-Rousan et.al., 2003), and the investigation concluded that the anomaly of $\delta^{18}O$ in seawater throughout the year is negligible for SST reconstruction. Sr/Ca around corals has not been monitored in all studies, and this study would be the first to revisit this assumption.

For the reconstruction of climate history using speleothems, it is most common to use $\delta^{18}O$ as a proxy to investigate past precipitation. In this methodology, there are also two assumptions: (1) $\delta^{18}O$ in rainwater, dripwater, and speleothems is continuously correlated, and (2) there is a predictable relationship between precipitation and $\delta^{18}O$ in rainwater called the *amount effect* (Dansgaard, 1964). The first assumption means that the value of $\delta^{18}O$ in rainwater is conserved in dripwater and speleothems. It is apparent that the $\delta^{18}O$ in speleothems originates from cave dripwater, which is the final product of rainwater. However, the hydrologic paths in the bedrock above the cave ceilings are complex. Residence and transit times may vary significantly, and some mixing can occur, so the age and origin of dripwater associated with different speleothems can vary even for coeval speleothem deposits. Cruz Jr. et al. (2005) reported that dripwater composition can vary depending on variations in rock cover thickness and drip hydrology characteristics. Regarding the second assumption, the amount effect is the observation that there is an inverse relationship between precipitation and $\delta^{18}O$ in rainwater. Therefore, it is possible to estimate the precipitation by measuring $\delta^{18}O$ in rainfall. In this study, $\delta^{18}O$ in rainwater and dripwater was measured to test these two assumptions. In addition, nitrate and alkalinity were measured to help us understand stalagmite calcification, because these elements are reported to affect stalagmite growth rate (cf., Hill, 1999, Genty et. al, 2001).

Understanding the growth process of speleothems is extremely useful information by which to better interpret speleothem calcification.

2.2 Methodology

2.2.1 Seawater

2.2.1.1 SST, $\delta^{18}O$ and Sr/Ca monitoring

One 4-ml vial for $\delta^{18}O$ and one 30-ml bottle for Sr/Ca have been collected monthly from September 2009 to present at Gabgab Beach, and from August 2009 to August 2010 at Haputo Bay (Figure 1). It is safe to swim year round at Gabgab Beach, so the seawater samples have been collected adjacent to the sample site. At Haputo Bay, however, it is dangerous to swim beyond the reef front, so the seawater sampling was conducted about 10 m seaward from the beach which is in line with the coral sample. A temperature logger, (TidBit HOBO), has been deployed at Gabgab Beach from September 2009 to January 2010 and from November 2010 to present. At Haputo Bay, it was deployed from August 2009 to February 2010. At the University of Texas, Austin (UTA), $\delta^{18}O$ was analyzed by Isotope Ratio Mass Spectrometry (IRMS), and Sr/Ca was analyzed by Inductively Coupled Plasma Optical Emission Spectrometer (ICP-OES).

2.2.1.2 Nitrate monitoring

One 50-ml bottle was collected at Gabgab Beach at least monthly from August 2009 to November 2010 right next to the coral sample. The sample was frozen right after the sampling to stop the biological activity, and then analyzed by Flow Injection Analysis (FIA) within 30 days from the sampling date at the WERI Water Chemistry Laboratory at the University of Guam (UOG). The methodology for seawater sampling is summarized in Table 1.

Table 1. Summary of seawater sampling methodology.

Type of water	**Sea water**					
Site	**Gabgab**			**Haputo**		
Chemical analysis	**$\delta^{18}O$**	**Sr/Ca**	**Nitrate**	**$\delta^{18}O$**	**Sr/Ca**	**Nitrate**
Container	4-ml glass vial	30-ml plastic	50-ml plastic	4-ml glass vial	30-ml plastic	50-ml plastic
Pre-treatment	none	2% HNO_3	frozen	none	2% HNO_3	frozen
Analysis	IRMS	ICP-OES	FIA	IRMS	ICP-OES	FIA
Sampling term	September, 2009-present		September, 2009-November, 2010	August, 2009-2010		

2.2.2 Cave dripwater

2.2.2.1 $\delta^{18}O$ monitoring

One 4-ml vial for $\delta^{18}O$ was collected monthly from September 2008 to present at nine sites in Jinapsan Cave (Partin et al., submitted). The cap was tightly closed in the cave and parafilmed to prevent evaporation. The samples were analyzed by IRMS at UTA.

2.2.3 Rainwater

2.2.3.1 $\delta^{18}O$ monitoring

One five-liter rainwater collection bottle with a funnel and filter was deployed at UOG. To prevent evaporation, 250 ml of mineral oil was poured in the collection bottle. Two 4-ml vials for $\delta^{18}O$ have been collected biweekly from September 2008 to present at UOG. The cap was tightly closed and parafilmed at UOG to prevent evaporation and analyzed by IRMS at UTA. The methodology for freshwater sampling is summarized in Table 2.

Table 2. Summary of freshwater sampling.

Type of water	**Rainwater**	**Dripwater**		
Site	**UOG**	**Jinapsan**		
Chemical Analysis	**$\delta^{18}O$**	**$\delta^{18}O$**	**Nitrate**	**Alkalinity**
Container	4-ml glass vial	4-ml glass vial	50-ml plastic	30-ml glass
Pre-treatment	none	none	frozen	crimping
Analysis	IRMS	IRMS	FIA	titration
Term	October 2009 - Present	September 2009 - Present		

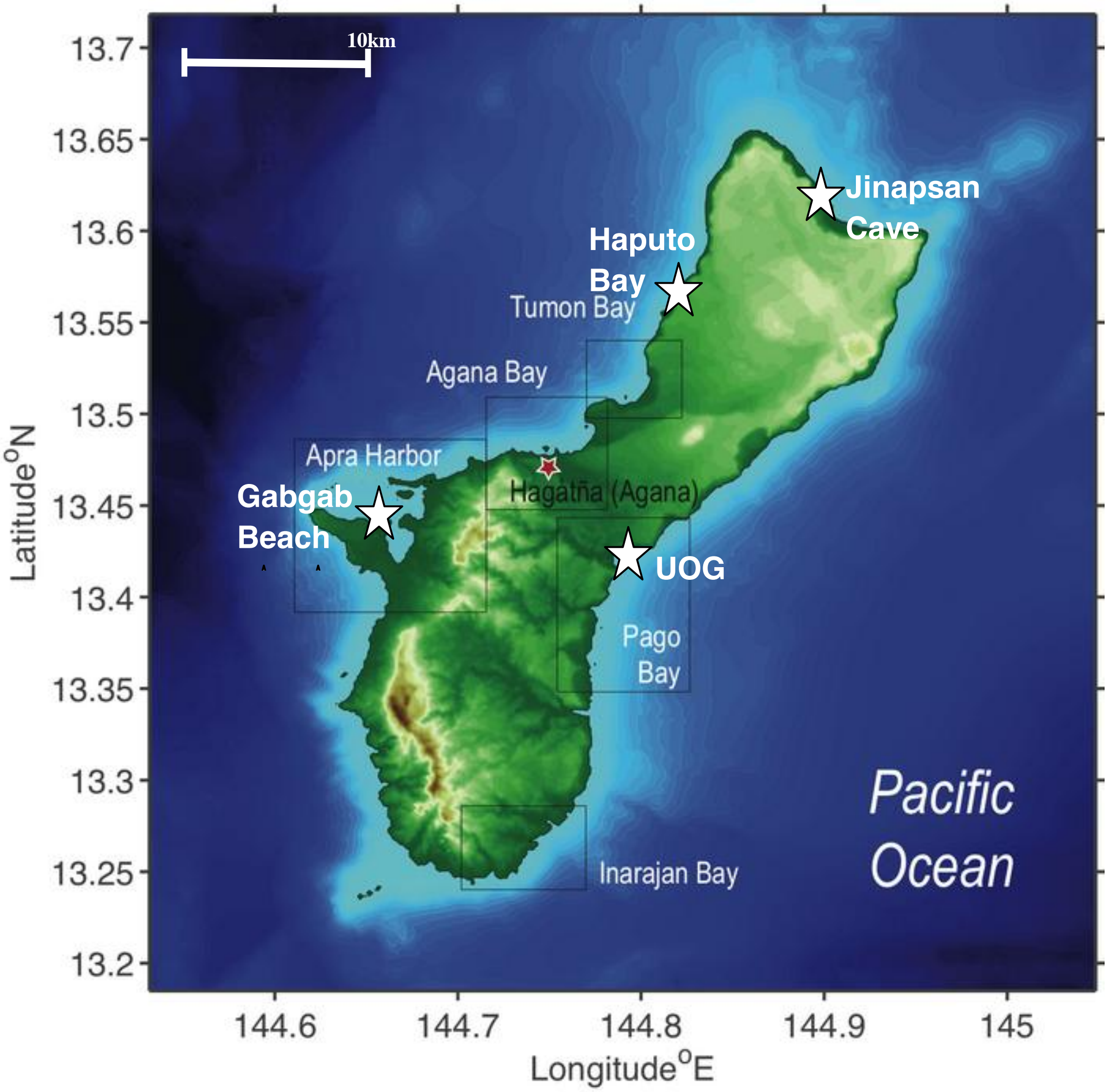

Figure 1. Locations of in situ monitoring: Jinapsan Cave, Haputo Bay, Gabgab Beach and UOG are shown by white stars. The original map is from NOAA website: http://nctr.pmel.noaa.gov/state/guam/.

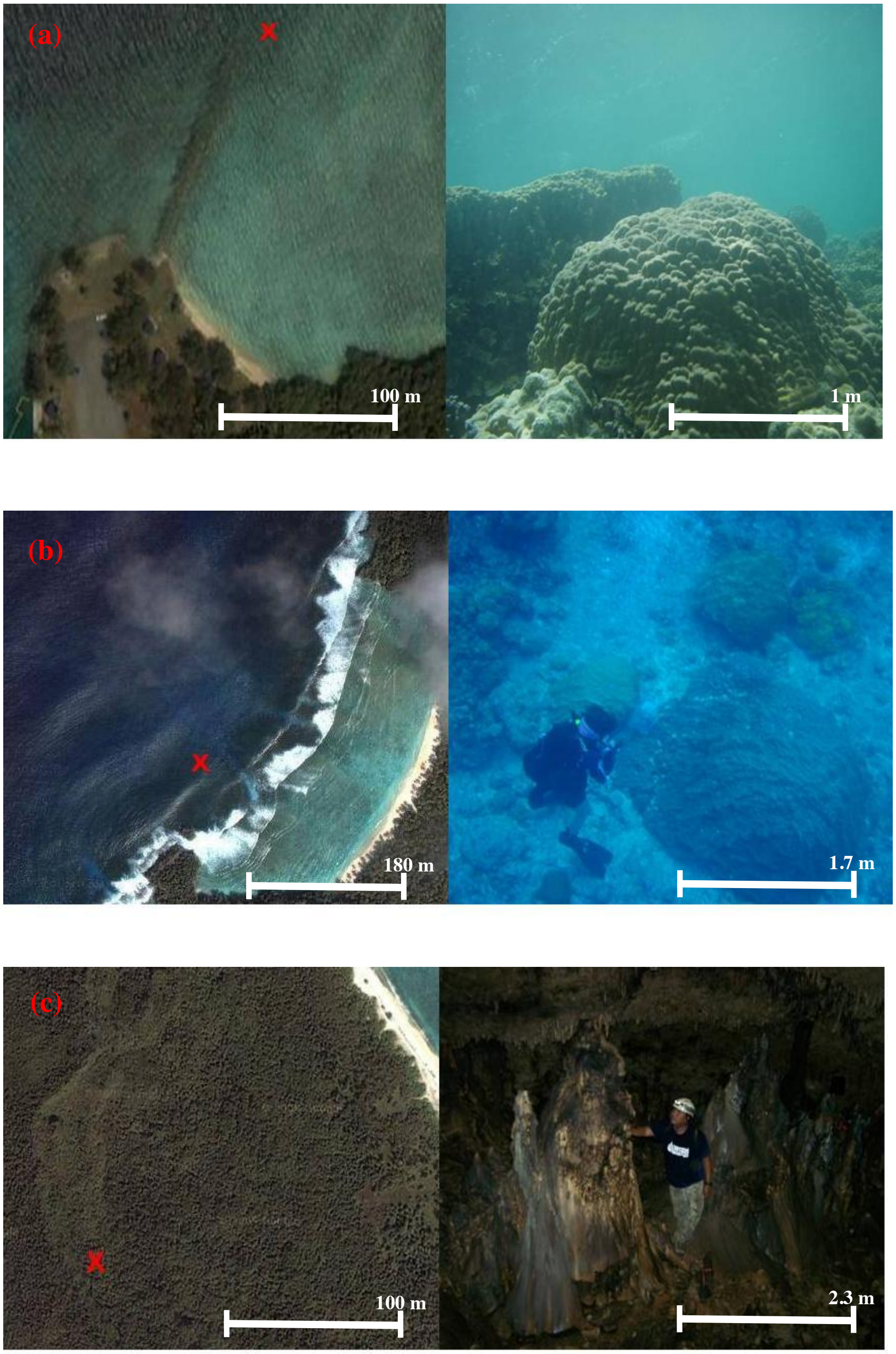

Figure 2. Photos of three study sites: (a) Gabgab Beach (b) Haputo Bay (c) Jinapsan Cave. Red X shows the approximate location of the sample at each site. The aerial photos are from Google maps website: http://maps.google.com/

2.3 Results

2.3.1 SST at Gabgab Beach and Haputo Bay

The correlation between Gabgab and Haputo SST from our temperature loggers was r = 0.98. Most significantly, they also correlated very closely with the Hadley SST dataset from MetOffice, UK. The correlations between Hadley SST and Gabgab and Haputo Bays were r = 0.93 and 0.98, respectively. The correlations with other public SST datasets were also investigated to identify the best long term data for coral geochemical analysis. This is discussed in section 4.0. Asami et al. (2005) assumed that Hadley SST is the best public dataset to compare with Guam coral geochemistry results, and our results (Figure 3) are consistent with their assumptions.

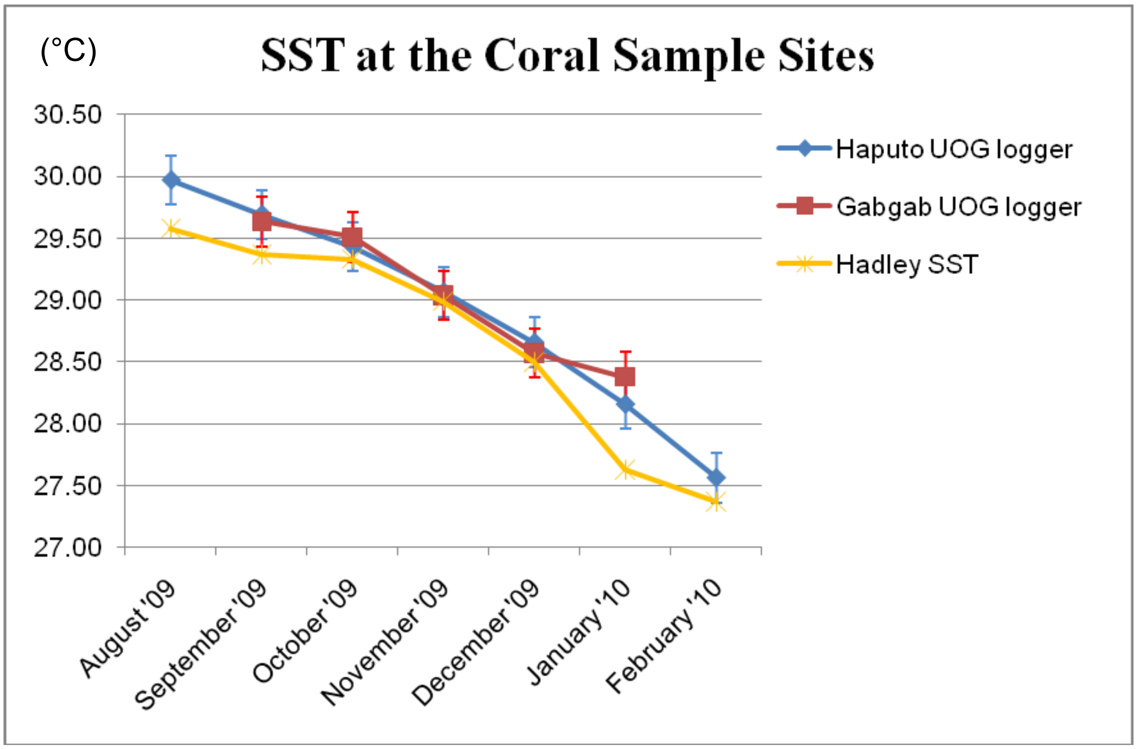

Figure 3. SST comparison between the UOG temperature logger from Haputo Bay, Gabgab Beach and Hadley SST data (˚C) based on monthly average. Error bars are ± 0.2˚C.

2.3.2 Seasonal pattern of seawater $\delta^{18}O$ at Gabgab Beach

Our time series for $\delta^{18}O$ seawater data will be posted in the NASA Global Seawater Oxygen-18 Database (http://data.giss.nasa.gov/o18data/). Seawater $\delta^{18}O$ showed seasonality, and it was highest in September and lowest in February (Figure 4). The average value was -0.52 ‰ relative to Vienna Standard Mean Ocean Water (VSMOW), with extremes at -0.3‰ to -0.7‰. Al-Rousan et al. (2003) reported that $\delta^{18}O$ shows a weak seasonality in the Red Sea, where salinity is the highest in the world: the average value was about 1.86‰, with a range from 1.75 ‰ to 2.0‰. In their study, they concluded that seawater $\delta^{18}O$ anomaly is negligible for SST reconstruction using $\delta^{18}O$ in corals. Our seawater $\delta^{18}O$ results are expectedly different from his study mainly because of the meteorological and geological differences. The climate around the Red Sea is continually dry while Guam has a distinct rainy season that can make the value of seawater $\delta^{18}O$ lighter. Rohling (2007) stated that seawater $\delta^{18}O$ varies due to evaporation, atmospheric vapor transport, precipitation and subsequent return of freshwater to the ocean. The value from our study matched well with the Global Surface Seawater $\delta^{18}O$ v1.19 (NASA, 2009), -0.5 ‰ to 0.5 ‰ around Guam. The result from December 2009 was off from the declining trend, showing the sea water $\delta^{18}O$ became lighter, which could be due to the heavy precipitation on December 2, 2009, brought by Tropical Storm Nida and tropical disturbance 97W (Figure 5). As these storms passed nearby, up to 11.95 inches of rain were recorded on Guam (Umatac rain gage) in 24 hours.

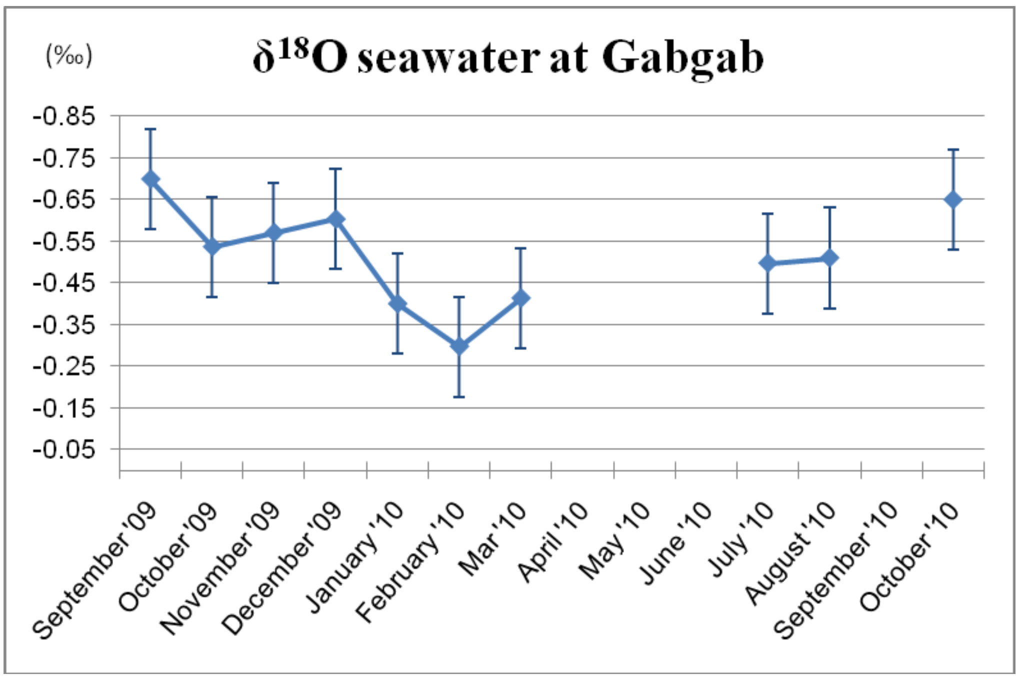

Figure 4. Seasonal variations in $\delta^{18}O$ seawater at Gabgab (‰ relative to VSMOW) at Gabgab based on monthly sampling. Error bars are $\pm$ 1σ.

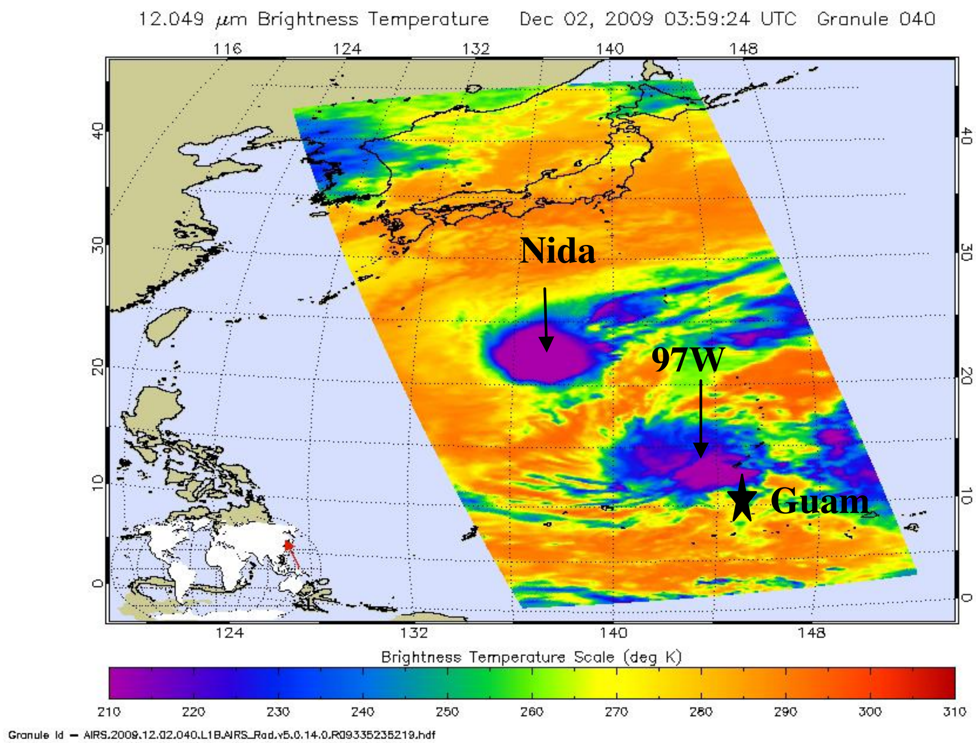

Figure 5. The unusually high daily precipitation caused by the nearby passage of Tropical Storm Nida and disturbance 97W on December 2, 2009, which brought up to 11.95 inches (Umatac rain gage) in 24 hours. Image from NASA (2010).

2.3.3 Temporal variability of Sr/Ca seawater at Gabgab Beach

There have been no previous studies that conducted time series of Sr/Ca seawater by monitoring around corals as all the studies strongly relied on the assumption: Sr/Ca in seawater is stable**.** Correge (2006) stated that variability in seawater Sr/Ca is far less than that of $\delta^{18}O$, so that is why Sr/Ca coral may be regarded as a "cleaner" proxy. Our Sr/Ca seawater analysis turned out to be a technically challenging task as it is hard to prepare the seawater standards for Sr and Ca. Kester et al., (1967) suggested the methodology to create artificial seawater that can be standard for this analysis. This seawater analysis is underway and will be completed upon the success of standard preparation.

2.3.4 SST vs seawater δ^{18}O at Gabgab Beach

It is believed that the main cause of seawater $\delta^{18}O$ variation is evaporation. Thus seawater $\delta^{18}O$ should be temperature and salinity-dependent, and each climate zone should show a characteristic value and seasonal variation of seawater $\delta^{18}O$. Al-Rousan et al. (2003) reported that there is strong correlation between salinity and seawater $\delta^{18}O$:

$$\textit{Seawater } \delta^{18}O \text{ (‰ VSMOW)} = 0.281 \times \textit{Salinity} - 9.14 \quad \textit{eqn. (1)}$$

In this study, we analyzed the correlation between SST and seawater $\delta^{18}O$ at Gabgab Beach. Figure 6 shows that there was a correlation with Hadley SST, (r = -0.88). Linear regression of seawater $\delta^{18}O$ against Hadly SST (Figure 7) shows that:

$$\textit{Seawater } \delta^{18}O \text{ (‰ VSMOW)} = -5.675 \times \textit{Temperature} + 25.521 \quad \textit{eqn. (2)}$$

The sampling has been continuing to present, so adding more data will make this relationship more reliable.

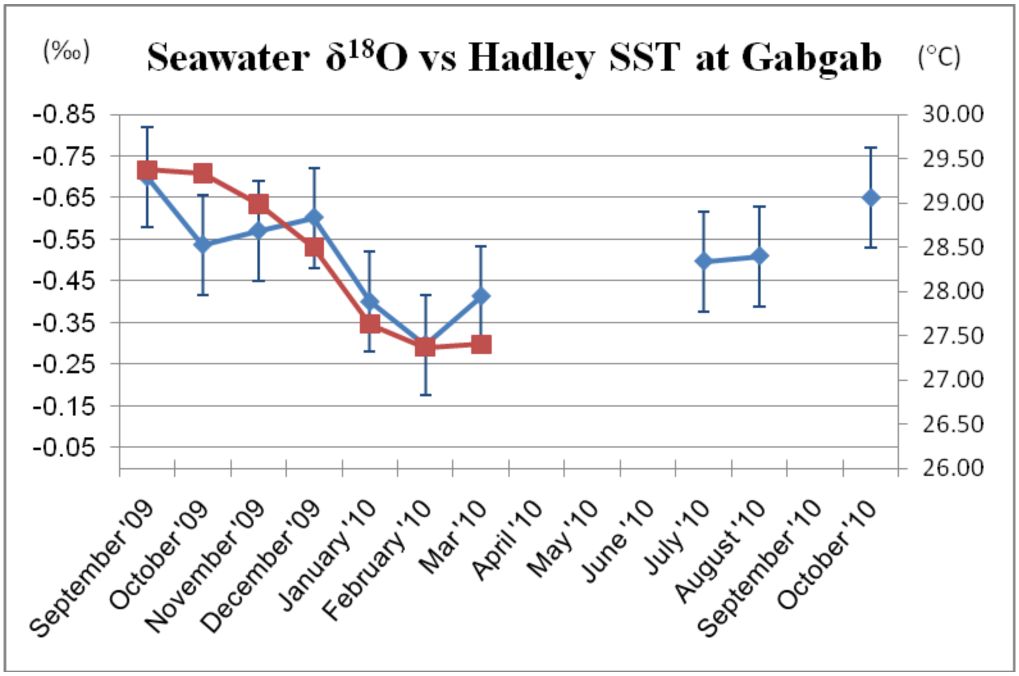

Figure 6. Time series comparison between seawater $\delta^{18}O$ at Gabgab (‰ relative to VSMOW) (blue line) based on monthly sampling and Hadley SST data (˚C) (red line). Error bars for isotope are ± 1σ.

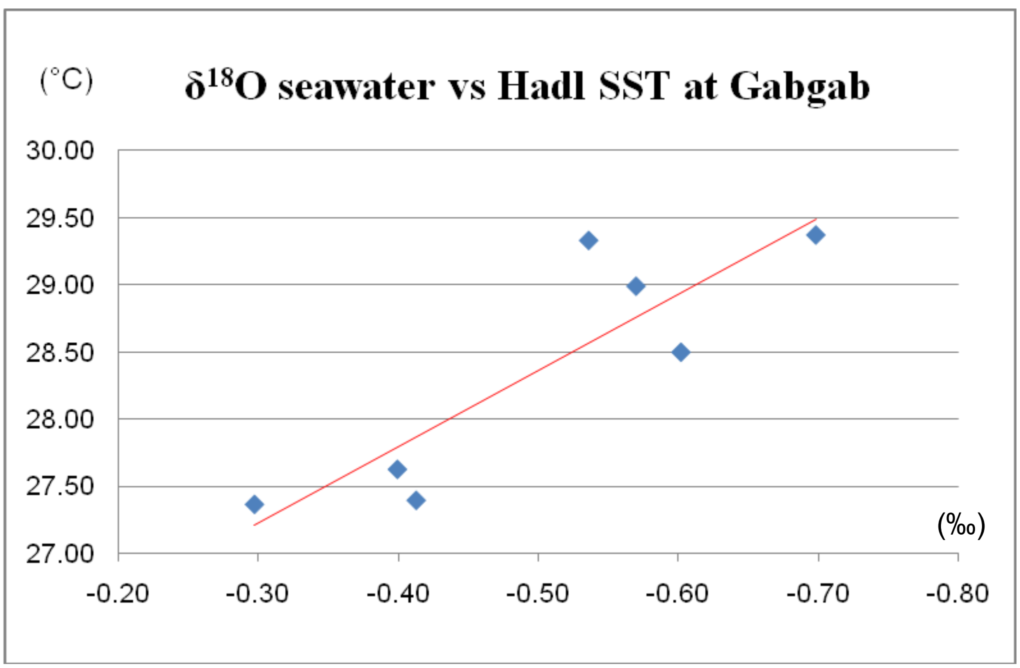

Figure 7. Correlation between seawater $\delta^{18}O$ at Gabgab (‰ relative to VSMOW) and Hadley SST data (˚C) based on monthly average from September 2009 to March 2010. Red line is the trend line.

2.3.5 SST vs seawater $\delta^{18}O$ at Haputo Bay

In contrast to Gabgab Beach, there was only weak correlation between SST and seawater $\delta^{18}O$ at Haputo Bay. (See Figure 8: r = 0.39). The average of seawater $\delta^{18}O$ was -0.517 ‰ at Gabgab Beach and -0.638 ‰ at Haputo Bay. This may be reflecting the influence of abundant fresh water discharge at Haputo Bay. Also, the affect of SST on seawater $\delta^{18}O$ seems to be hidden: fresh water influence is larger than temperature influence at this site.

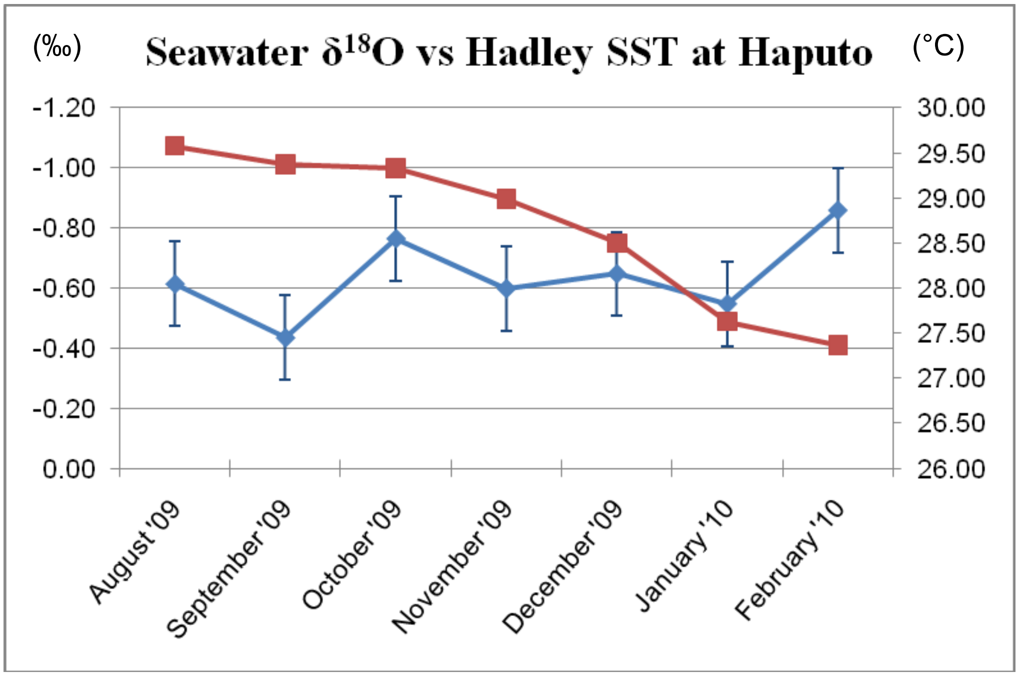

Figure 8. Time series comparison between seawater $\delta^{18}O$ at Haputo (‰ relative to VSMOW) (blue line) based on monthly sampling and Hadley SST data (˚C) (red line). Error bars for isotope are ± 1σ.

2.3.6 Seawater $\delta^{18}O$ vs rainwater $\delta^{18}O$

To gain insight into how $\delta^{18}O$ varies in the different components of the local hydrologic system, we compared local seawater $\delta^{18}O$ to local rainwater $\delta^{18}O$ (Figure 9). There was strong correlation (r = 0.90). Figure 10 shows the linear relation:

$$\delta^{18}O\ seawater = 0.0633 \times \delta^{18}O\ rainwater\ -0.3131 \quad eqn. (3)$$

In Guam, the local precipitation is affected by the moisture traveling from subtropical (e.g., Hawaiian region) due to trade winds, but this result is showing that evaporation in the local ocean may possibly contribute to the precipitation in Guam.

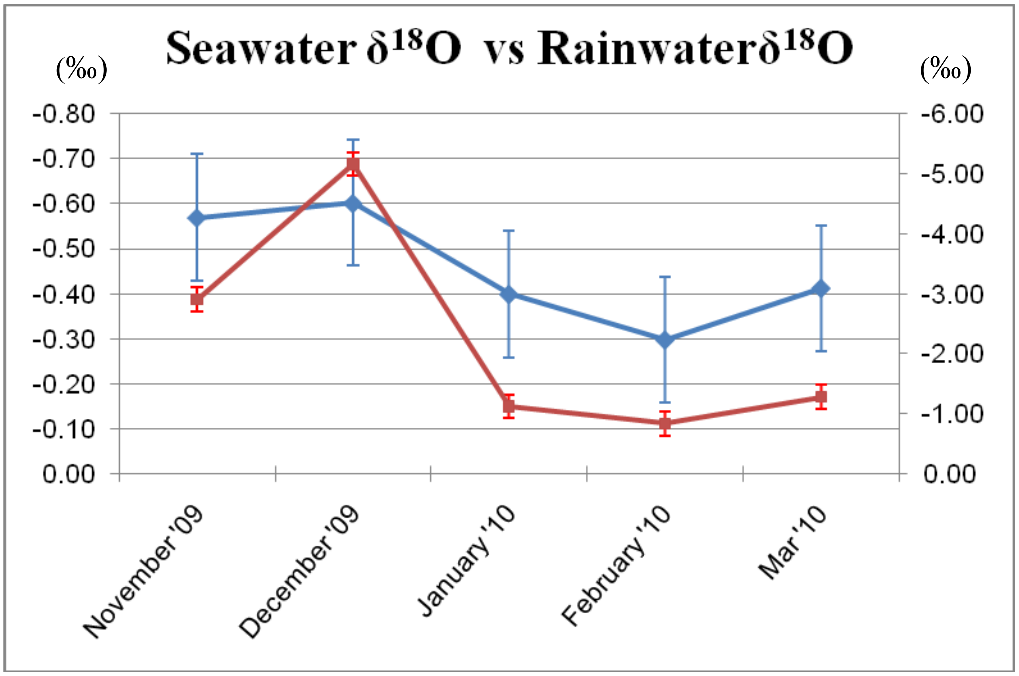

Figure 9. Time series comparison between seawater $\delta^{18}O$ at Gabgab (‰ relative to VSMOW) (blue line, left-side scale) based on monthly sampling and rainwater $\delta^{18}O$ at UOG (red line, right-side scale) based on biweekly sampling. Error bars are ± 1σ (Partin et al., submitted).

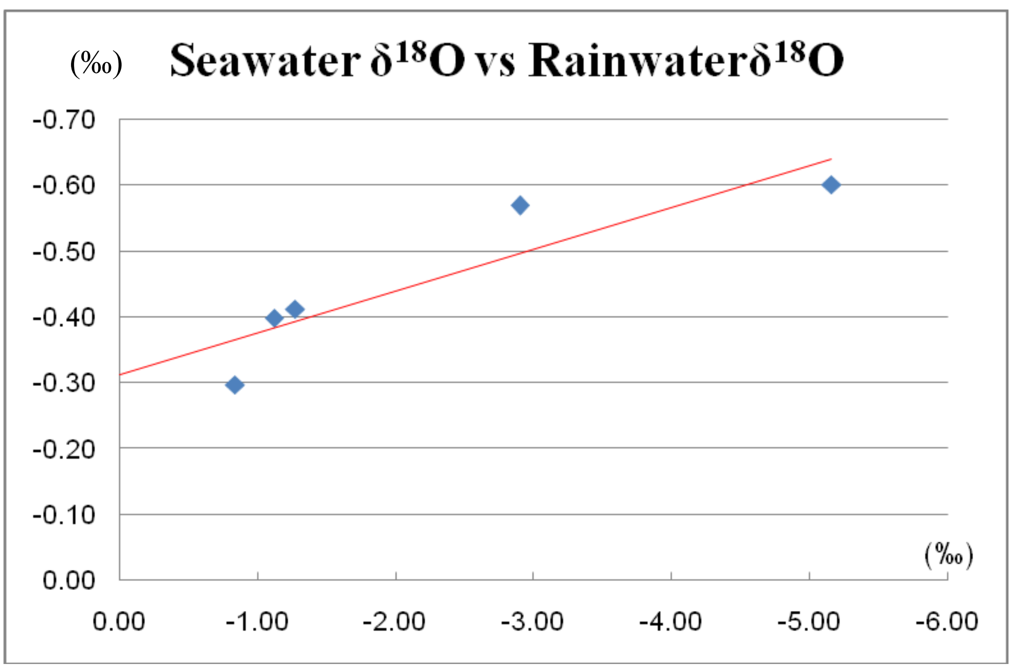

Figure 10. Correlation between $\delta^{18}O$ seawater at Gabgab (‰ relative to VSMOW) based on monthly average and $\delta^{18}O$ rainwater at UOG (‰ relative to VSMOW) based on biweekly average. Red line is the trend line.

2.3.7 Rainwater $\delta^{18}O$ vs precipitation

Rain gauge data between UOG and seven rain gauge stations were compared, and all the stations showed strong correlation each other (r > 0.8) as shown in Table 3. To test the amount effect, we compared rain gauge data from eight sites on Guam (Figure 11) to rainwater $\delta^{18}O$ from our UOG rainwater collection station. The precipitation from six stations: UOG, Mt. Chaochoa near Piti, Fena at Nimitz Park, Mt. Santa Rosa, Windward at Talofofo, and Andersen Air Force Base, showed strong correlation (r < -0.79) based on cross correlation test shown in Table 4. Two stations, Almagosa near Naval Magazine and Mt. Santa Rosa showed low correlation (r = -0.554 and r = -0.016, respectively). From this result, the amount effect was verified at UOG station and indirectly confirmed at five stations on the island. However, the amount effect could not be confirmed with available data at two stations even though their rain data highly correlates with UOG station. This could be due to the dataset missing data points during wet season which are necessary to establish the strong trend seen at UOG Station.

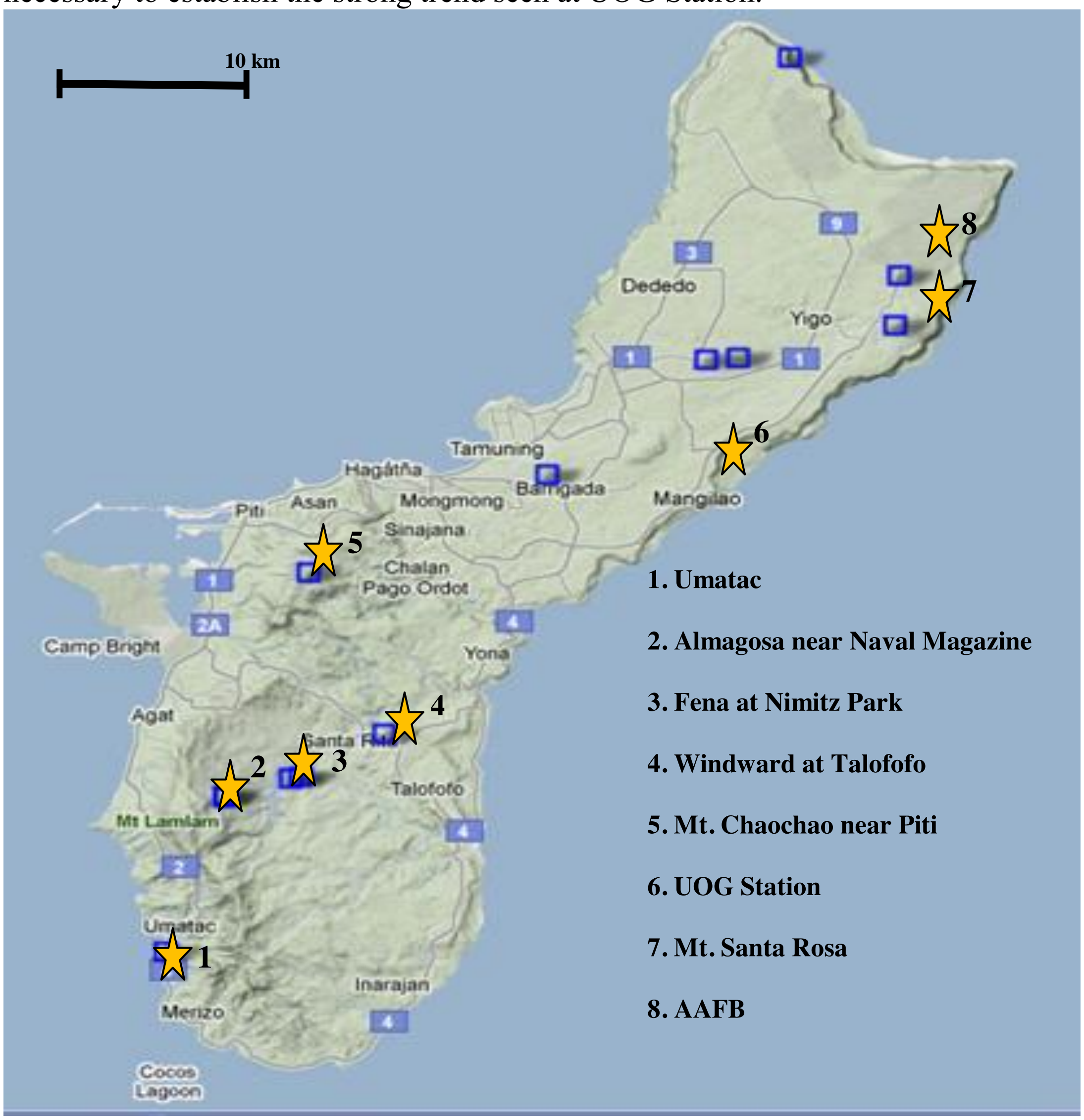

Figure 11. Eight rain gauge stations used in this study. The original map is from USGS website: http://wdr.water.usgs.gov/nwisgm ap/?state=gu

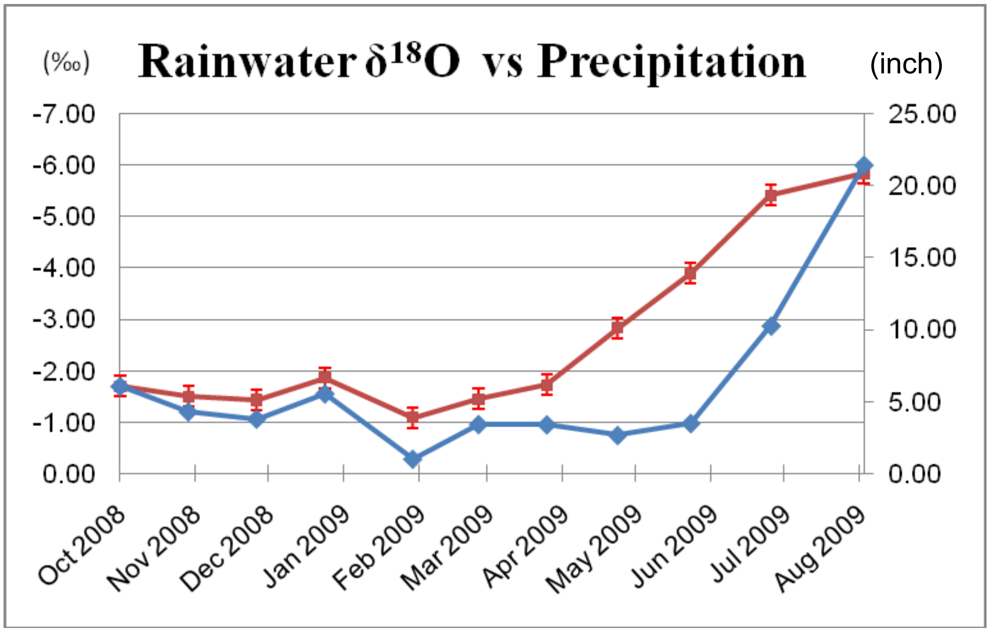

Figure 12. Comparison between rainwater $\delta^{18}O$ (‰ relative to VSMOW) (red line) based on biweekly average and monthly total precipitation from UOG station (inch) (blue line). Error bars for isotope are ± 1σ, see Partin, et al., submitted.

Table 3. Cross correlation test between monthly total precipitation at UOG Station and seven rain gauge stations on Guam

		UOG Station
Almagosa near Naval Magazine	r	0.800
	p	0.005
Mt. Chachao near Piti	r	0.991
	p	<0.001
Fena at Nimitz Park	r	0.982
	p	<0.001
Mt. Santa Rosa	r	0.967
	p	<0.001
Windward at Talofofo	r	0.996
	p	<0.001
Umatac	r	0.965
	p	<0.001
AAFB	r	0.988
	p	<0.001

Table 4. Cross correlation test between rainwater $\delta^{18}O$ from UOG Station and monthly total precipitation at eight rain gauge stations on Guam.

	Almagosa near Naval Magazine	Mt. Chachao near Piti	Fena at Nimitz Park	Mt. Santa Rosa
r	-0.554	-0.885	-0.794	-0.016
p	0.096	0.008	0.003	0.970
	Windward at Talofofo	Umatac	UOG Station	AAFB
r	-0.855	-0.797	-0.852	-0.791
p	0.001	0.003	0.001	0.004

2.3.8 Precipitation vs. cave dripwater $\delta^{18}O$

We note here that the seasonal rainfall $\delta^{18}O$ signal reported above is being found in cave dripwaters in an ongoing complementary study of the dripwater and speleothem chemical records in Jinapsan Cave, located on northern Guam. Partin et al. (submitted) report that cave dripwater $\delta^{18}O$ from two stations, Station 1 and Stumpy, shows not only a distinct seasonal variability, but inter-annual variability as well (Figure.13). It is also apparent that dripwater residence times and mixing rates vary from site to site: while these two stations are successfully preserving the present rainwater $\delta^{18}O$ in their dripwater, the other six stations (Figure 14), Station 2, Stumpy Brother, Station 4, Flatman, Borehole and Trinity, are not reflecting an obvious relationship to rainwater $\delta^{18}O$. The fact that seasonal signals are indeed present in some to the dripwaters of the cave, however, leaves open the possibility that such annual variations could also be found in suitably fast-growing speleothems in the cave. (We have yet to find these, however.) If so, we may eventually be able to correlate and calibrate local speleothem records with local coral records. A detailed description of the results of the cave study to date is given by Partin et al. (submitted).

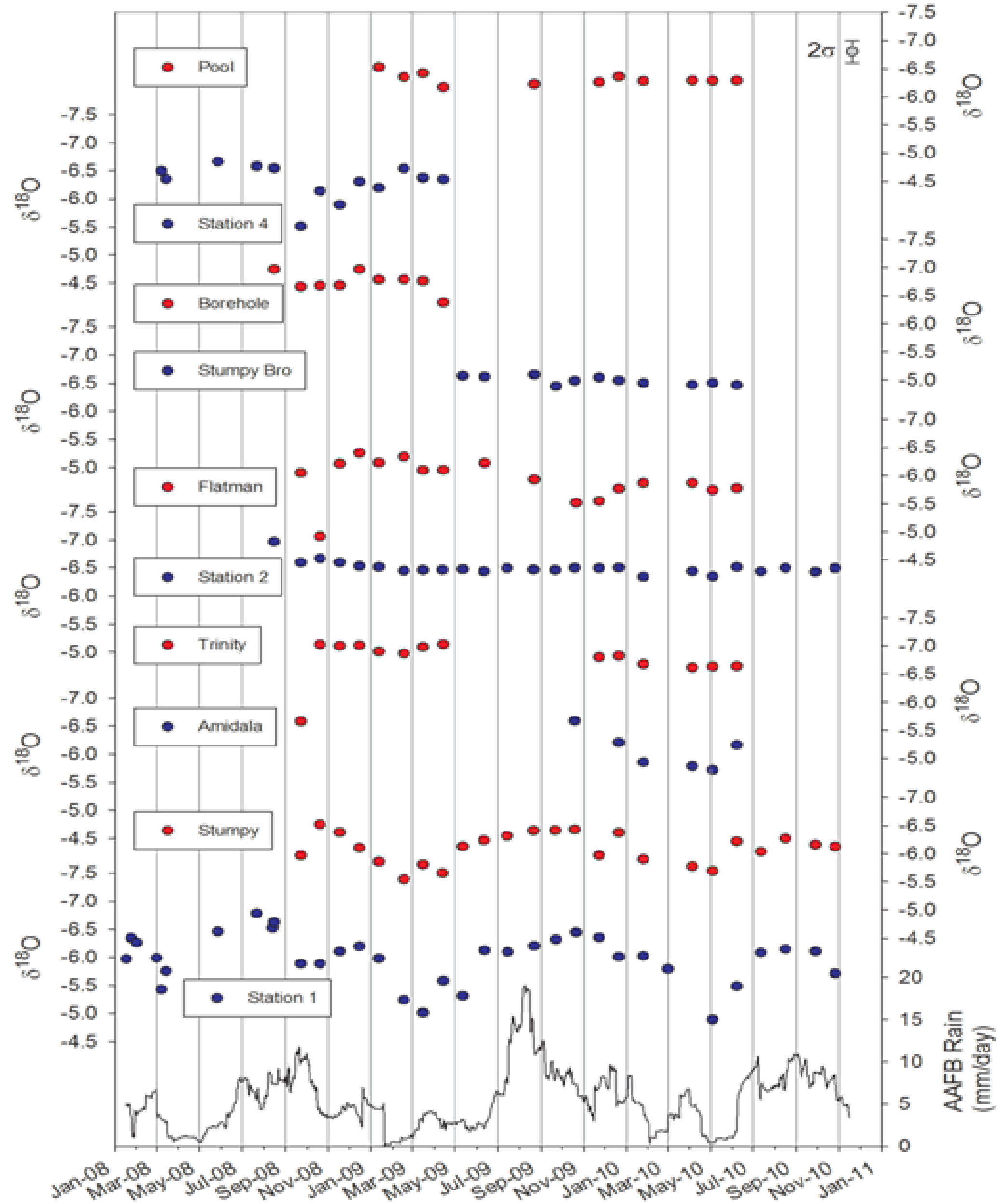

Figure 13. Comparison between precipitation (mm/day) and dripwater $\delta^{18}O$ (‰ relative to VSMOW) at the nine stations and brackish pool in Jinapsan Cave. The graph is quoted from Partin et al. (submitted).

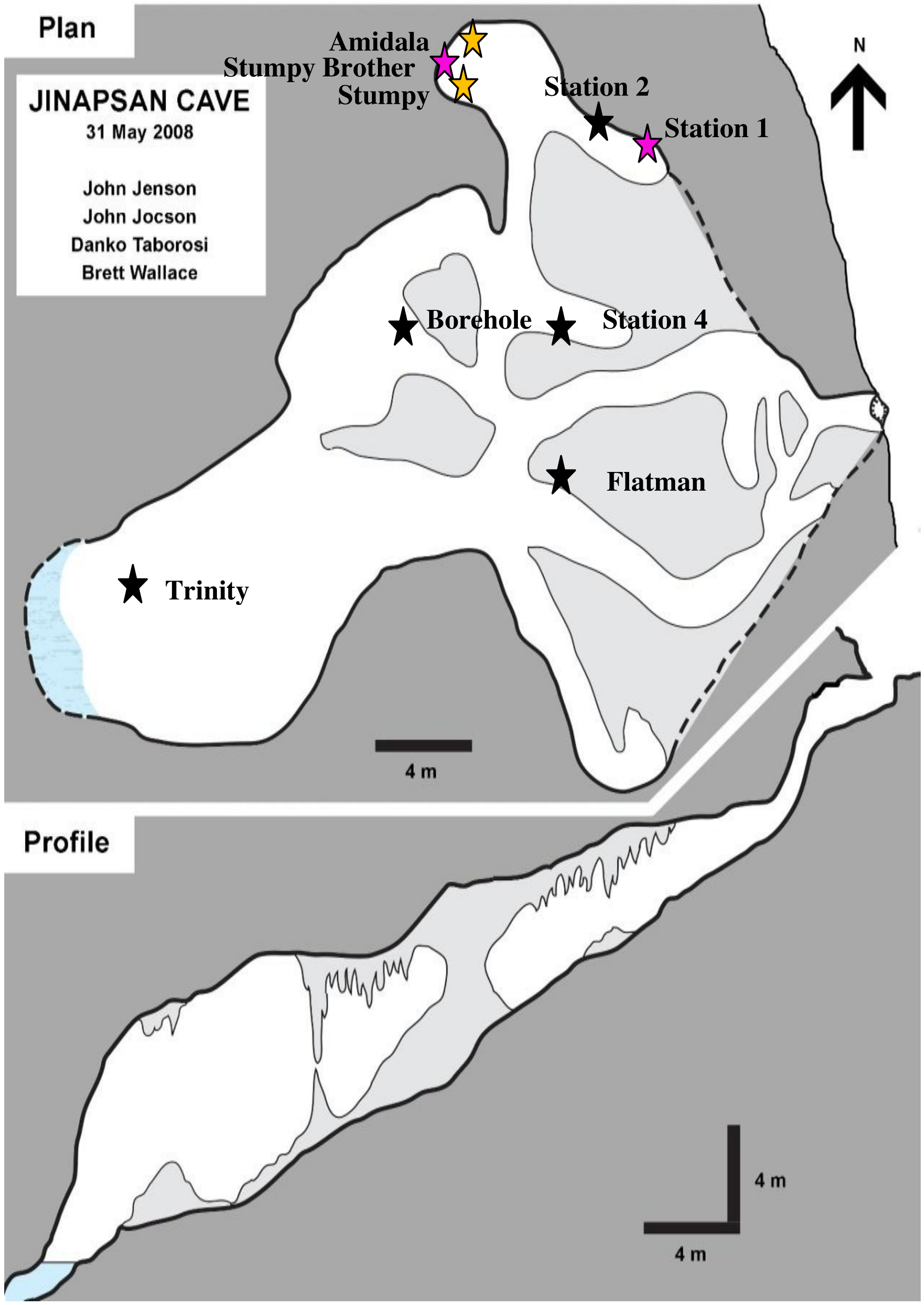

Figure 14. Jinapsan Cave. Pink stars show the stations showing correlations between precipitation and cave dripwater $\delta^{18}O$ and black stars show the stations showing no correlations. Yellow stars show the stations that need more samples for this analysis.

2.3.9 Nitrate in seawater vs precipitation

Marubini and Davies (1996) reported that a high nitrate level reduces coral calcification because the number of algae cells in corals, zooxanthellae, increases with higher levels of nitrate, and take over the carbon intake by photosynthesis. Their laboratory experiment using *Porites* proved that 1µM/L of nitrate, 0.062 mg/L, will dramatically reduce skeletogenesis in corals. Our results showed that the sample at Gabgab Beach, experienced a significant variation in nitrate level through the year, ranging from 0.01 to 0.06 mg/L, but not high enough concentration to affect coral calcification. In comparison, Yap et al. (2005) reported that the nitrate level of surface water in the west coast of Malaysia varied from 0.17 to 0.88 mg/L. Our result showed much lower concentration and variation.

At first, this nitrate anomaly was hypothesized to change due to precipitation. However, the correlation with nitrate and precipitation from the Piti rain gauge station, closest station to Gabgab Beach, which had available data from September 2009 to 2010, was weak (r = 0.45). After May the nitrate level was below detection level.

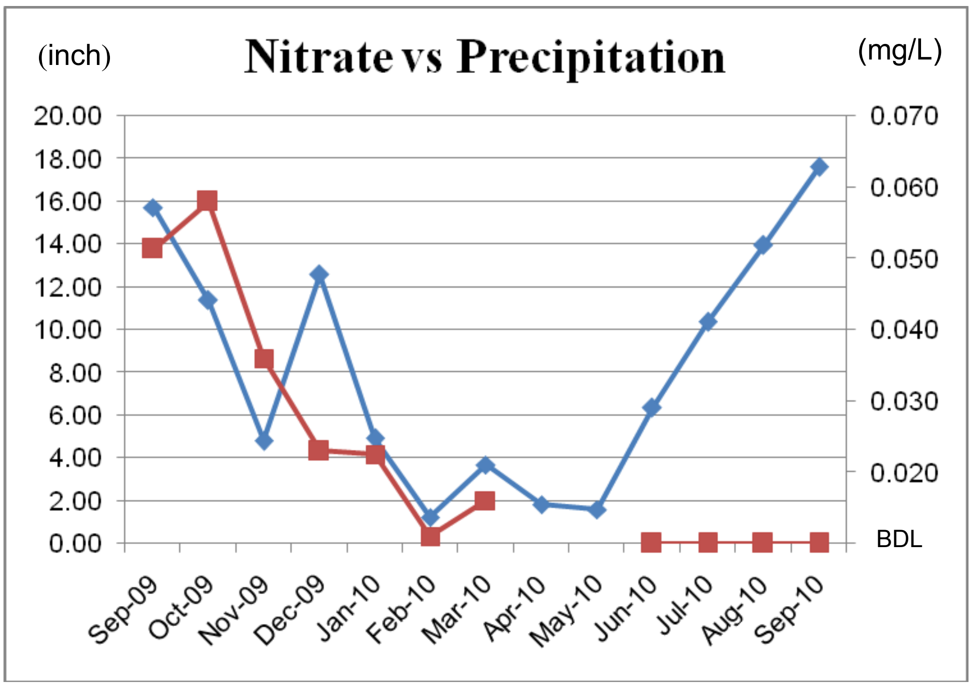

Figure 15. Comparison between nitrate in seawater from Gabgab (mg/L) (redline) based on monthly sampling and monthly total precipitation (inch) (blueline) at Piti. Analytical error for nitrate analysis is within 0.0008mg/L.

2.3.10 Nitrate in seawater vs SST

Wafar (1990) stated that the nitrate level around coral reefs is relatively greater than in adjacent ocean waters due to nitrification. Nitrifers, the aerobic bacteria responsible for nitrification, are known to work better when SST is higher. The reaction:

$$NH_3 + O_2 \rightarrow NO_2^- + 3H^+ + 2e^- \quad eqn\ (4a)$$

$$NO_2^- + H_2O \rightarrow NO_3^- + 2H^+ + 2e \quad eqn\ (4b)$$

is stimulated by higher SST. Carlucci and Strickland (1968) extracted nitrifers from the Pacific Ocean, and concluded that the optimal temperature for nitrifers is 28˚C.

To investigate the nitrate variation around the samples, nitrate level was compared to SST. There was a very strong correlation between these two, ($r = 0.90$, $p = 1.028E-15$), from October 2009 to March 2010 at Gabgab Beach (Figure 16). However, as previously mentioned, nitrate level dramatically dropped and became below detection level (0.01 mg/L) from May 2010, and remained at that level (Figure 15 & 16). Therefore, nitrate level and SST appear to be correlated for the part of the study interval. It seems that there are other possible factors that affect nitrate level around corals besides precipitation and SST.

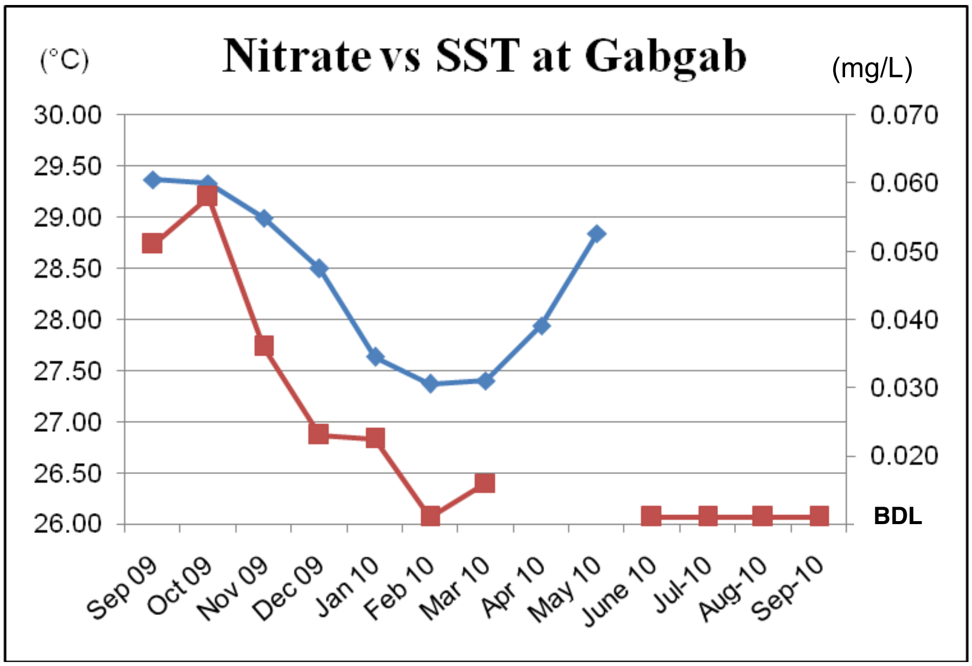

Figure16. Correlation between Nitrate at Gabgab (mg/L) based on monthly sampling (red line) and Hadley SST data (˚C) (blue line) based on monthly average. Analytical error for nitrate analysis is within 0.0008mg/L.

2.3.11 Nitrate in cave dripwater

High nitrate levels of more than 2.0 mg/L were found at Flatman and Trinity stations. These two stations were selected for this analysis as they are the only stations that yielded water in excess of our other sampling needs, which we otherwise discarded. For comparison, Jiménez-Sánchez et al. (2008) reported the mean nitrate level in a cave they studied in Spain was 1.07 mg/L from 2003 to 2004, and it was 2.70 mg/L from 2004 to 2005. They attributed this to an increase of surface contamination around the cave. To our knowledge, there has been no study to date as to what level of nitrate affects the bacteria that might affect speleothem calcification. Nevertheless, this analysis provides baseline data for future studies of this and related questions at Jinapsan Cave.

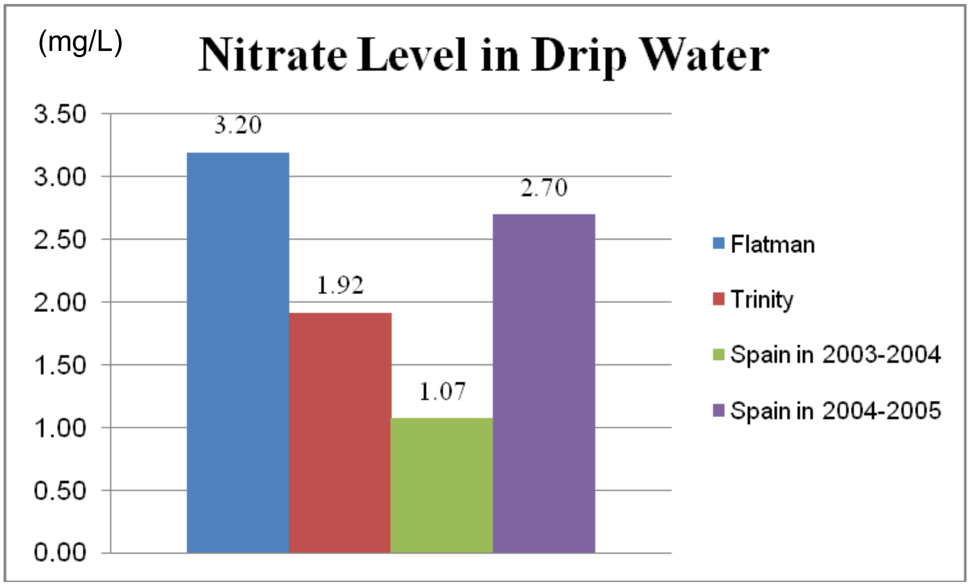

Figure 17. Mean nitrate level (from July to November 2010) in cave dripwater from Flatman and Trinity station in Jinapsan Cave. The values from Jiménez-Sánchez et al. (2008) (Spain) are shown for comparison. Analytical error for nitrate analysis is within 0.0008mg/L.

2.3.12 Alkalinity in cave dripwater

Alkalinity from the two stations, Flatman and Trinity, were compared as these were the only stations where we could consistently collect sufficient samples for this analysis. From February 2009 to June 2010 the alkalinity level was consistently higher at Flatman. Trinity has the fastest drip rate in Jinapsan Cave (21-79 drips per minute) and Flatman is much slower (2.5-6 drips per minute) based on the data from January to December 2009. Also, there was no correlation between alkalinity level and precipitation ($r = 0.23$ with Flatman, $r = 0.33$ with Trinity). The slow drip rate may be contributing to higher alkalinity levels at Flatman. Assuming that higher alkalinity helps stalagmites grow faster, and if Flatman successfully preserved precipitation signals in its dripwater $\delta^{18}O$, this station could be a great candidate for modern climate study.

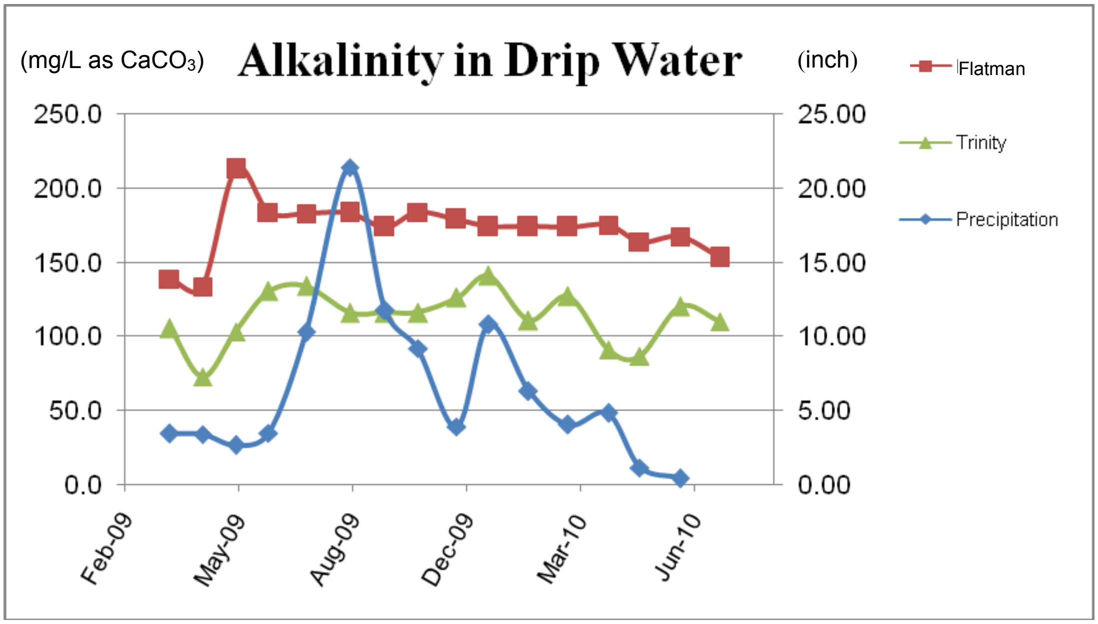

Figure 18. Alkalinity level at Flatman (red line) and Trinity stations (green line) (mg/L as $CaCO_3$) and precipitation (inch) (blue line).

2.4 Discussion

The sample at Gabgab Beach shows a high seasonal variation in SST, $\delta^{18}O$ and nitrate. Notably, even though Gabgab Beach is in a harbor, the SST record from the logger attached to the sample is very closely correlated with the Hadley SST dataset which is used for off-shore studies. Therefore, the Hadley SST dataset was identified as an adequate SST reference for this project. From our *in situ* monitoring, seawater $\delta^{18}O$ at Gabgab Beach was shown to respond to the SST signal. The correlation between $\delta^{18}O$ seawater and SST at the Gabgab Beach coral site suggests that the corals at this site are suitable for SST reconstruction study.

In addition, from this study we observed that the nitrifers in seawater at Gabgab Beach exhibits complex responses to SST and precipitation. Even though there is some variability shown in the sample at Gabgab Beach, it appears the range of concentration is not high enough to affect coral calcification. Thus, the biological effects which can disturb SST reconstruction seem to be negligible for the coral at Gabgab Beach.

From our long term *in situ* seawater, rainwater and cave dripwater $\delta^{18}O$ monitoring, we could align and correlate six environmental and geochemical factors on Guam: (1) SST around the coral at Gabgab Beach, (2) Hadley SST dataset, (3) seawater $\delta^{18}O$ around the coral at Gabgab Beach, (4) rainwater $\delta^{18}O$ from UOG Station, (5) precipitation from six rain gauge stations and (6) dripwater $\delta^{18}O$ at two stations in Jinapsan Cave. The coral at Haputo Bay and six of the dripwater stations in Jinapsan Cave were excluded because other hydrogeological factors, such as fresh water intrusion, appear to be affecting the climate signal. These selected coral and speleothem samples have proven to be the best for climate study on the island as is discussed below in section 5.0.

In Jinapsan Cave the Trinity and Flatman sites exhibit a very high level of nitrate. A preliminary analysis of rainwater collected from August to October 2010 right above

Jinapsan Cave had a nitrate level of ~0.02 mg/L. This suggests the source must be from the surface soil, the bedrock above the cave or some other source of groundwater seepage. No matter what the source, this high level of nitrate suggests that the mineralization of Trinity and Flatman may be affected by microbiological activity.

3.0 Exploration of the coral core sampling method

3.1 Introduction

For this study, we found it necessary to develop a new methodology for underwater drilling; a low-cost, easily portable underwater drill for obtaining coral core samples in shallow water (Bell et al., 2011). This proved very successful, and the drill itself thus constitutes a significant advance in the technology and methodology for this type of research. Coral core sampling methods have been developed since the late 1980's (cf., Easton, 1981, Isdale and Daniel, 1989; Kan et al., 1998). There are three common methods for underwater drilling: (1) hydraulic (2) pneumatic and (3) electric. Since coral doesn't grow completely vertical to the sea floor, coral cores for paleoclimate studies should be about 80 mm in diameter in order to contain the full, consecutive record along the coral growth axis. Given this width of core, the hydraulic drill is the most popular method to extract the core because of its power and high torque. However, Adachi and Abe (2003) noted that hydraulic drills are expensive and inconvenient to transport; they usually cost about $12,000 and weigh 1000 kg or more. Moreover, hydraulic drills require longer setup time and skilled operators. To overcome all these disadvantages of hydraulic drills, Adachi and Abe (2003) invented a pneumatic drill which can drill coral cores up to 10 m long and 55 mm in diameter. His drill costs about $2,000 and can be packed in two suitcases for remote sampling. The air source for his drill is common scuba tanks. This technology, however, requires scuba tank changes underwater and extra trips to the surface to send up segmented coral cores. With current methods, it is common to deliberately break the core to extract it. This requires divers to make repeated trips to surface, thus requiring longer diving time and more time on site.

Inspired by Adachi's pneumatic drill, and mindful of these sorts of limitations with the current technology, we decided to pursue a pneumatic drill able to extract a core 80 mm in diameter without requiring the breaking of coral cores or using scuba tanks. The most innovative characteristics of this drill are: (1) using an air motor instead of a regular pneumatic drill to deliver higher torque (2) using an air compressor aboard the boat instead of scuba tanks to send continuous air to the drill, and (3) using modular coring tubes to retrieve cores. In the current available methods, all the pneumatic drills have only one handle, making it difficult for the driller to drill vertically. Using an air motor with two handles gives not only higher torque but also greater stability underwater. Replacing scuba tanks with an air compressor eliminates the changing of tanks underwater, and lets the driller adjust the volume of air flow. Modular core tubes are easily attached or detached, depending on the length of the core, by using two custom wrenches. Furthermore, our toolkit included a core guide to stabilize the drill bit. There are two critical factors for drilling efficiently: (1) washing the core bit continuously and (2) getting rid of drilling debris. In our method, we used a pneumatic drill with a water pump to send sea water to the core bit and purge debris. The water pump is connected to the air compressor, so it didn't require an extra device.

3.2 Methodology

3.2.1 Finding the engineer

Five geological equipment suppliers specializing in drilling were contacted in Japan and the United States. The overview of the project, coral sample information and the ideas of the customized drill were explained by e-mail. One company didn't respond, another rejected the idea of detachable core tubes, and two others didn't think it was feasible to build a pneumatic drill that can extract a core with 80 mm in diameter. One company in Japan agreed to make a customized drill that met our requirements. They suggested that the widely-used hand-held pneumatic drill should be replaced with an air motor.

3.2.2 Making blueprints

The blueprints for the drill and accessories are shown in Figure 19. (See Bell et al., 2011, for details.) The drill bit was designed to be 70 mm long since the initiation of the drilling is the most difficult step, and the short drill bit would make the initial stage of drilling more stable and effective. There are three modular coring tubes, each 310 mm long, which can be coupled and decoupled. The most important part, the air motor, was chosen from Japan (Meiyu DF-67-093). The specifications for the air motor are 0.6 megapascals (Mpa) and 350 revolutions per minute (RPM). As accessories, a "core catcher" and a "core breaker" were designed for use as a backup in case the coral core was not able to be retrieved when the driller extracted the drill. The core catcher can be used to pinch and pull the core sample, and the core breaker can be used to peel off the core sample from the coral body itself. Adachi and Abe (2003) introduced a narrow stick called a "core breaker" to break the core after drilling. Unlike his core breaker, ours is a half circle to prevent the core from being broken internally.

3.2.3 Selecting a gasoline-powered air compressor

The air motor requires a constant, strong air flow from the compressor. A portable gasoline-powered air compressor within the weight and size capacity of the boat was not available on the island so an 8-gallon, two-stage air compressor (AM2-PH09-08M, Mi-T-M Corporation) was selected and ordered from the US mainland. The specification of this compressor is 17.2 cubic feet per minute (cfm) at 175 pounds per square inch (psi), and these are the minimum requirements for the air motor.

3.2.4 Testing on land

Before conducting underwater drilling, we conducted three types of tests: (1) checked the RPM and torque without any extension tubes (2) added one and two extension tubes to see if it made a difference in the RPM and (3) drilled a concrete block assumed to be harder than live coral.

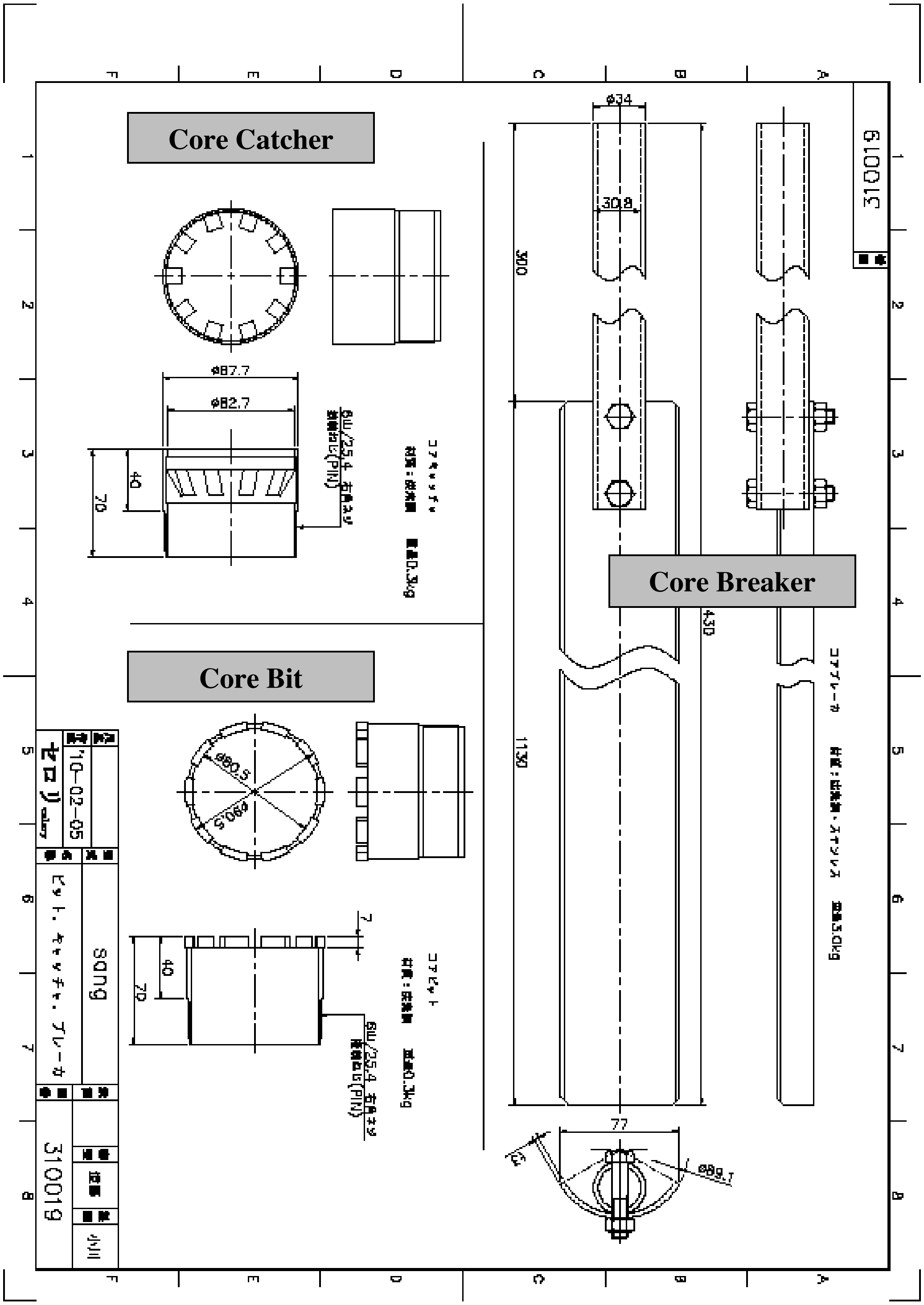

Figure 19 (a). Blueprint for the drill: core bit, core catcher and core breaker.

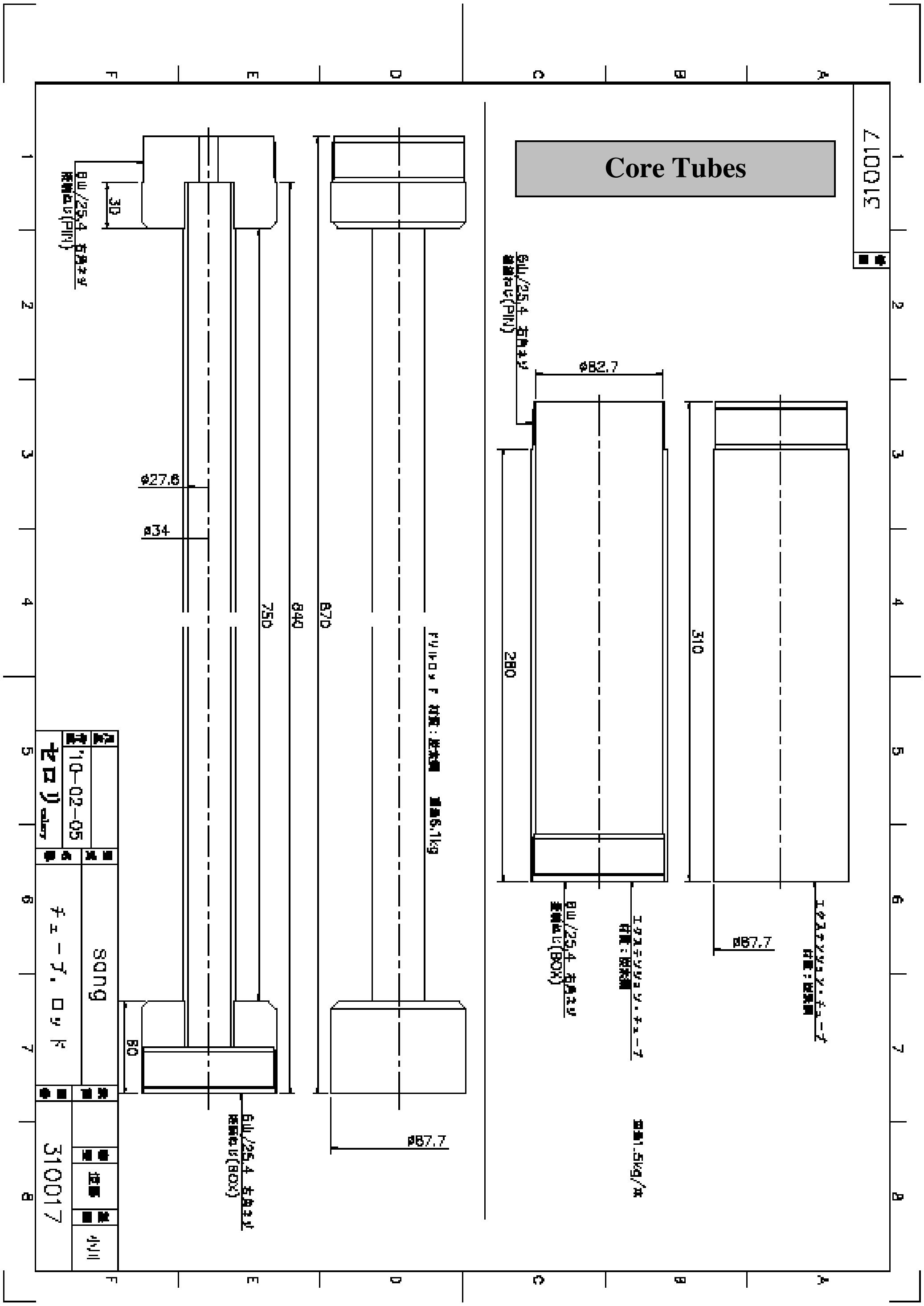

Figure 19 (b). Blueprint for the drill: core tubes.

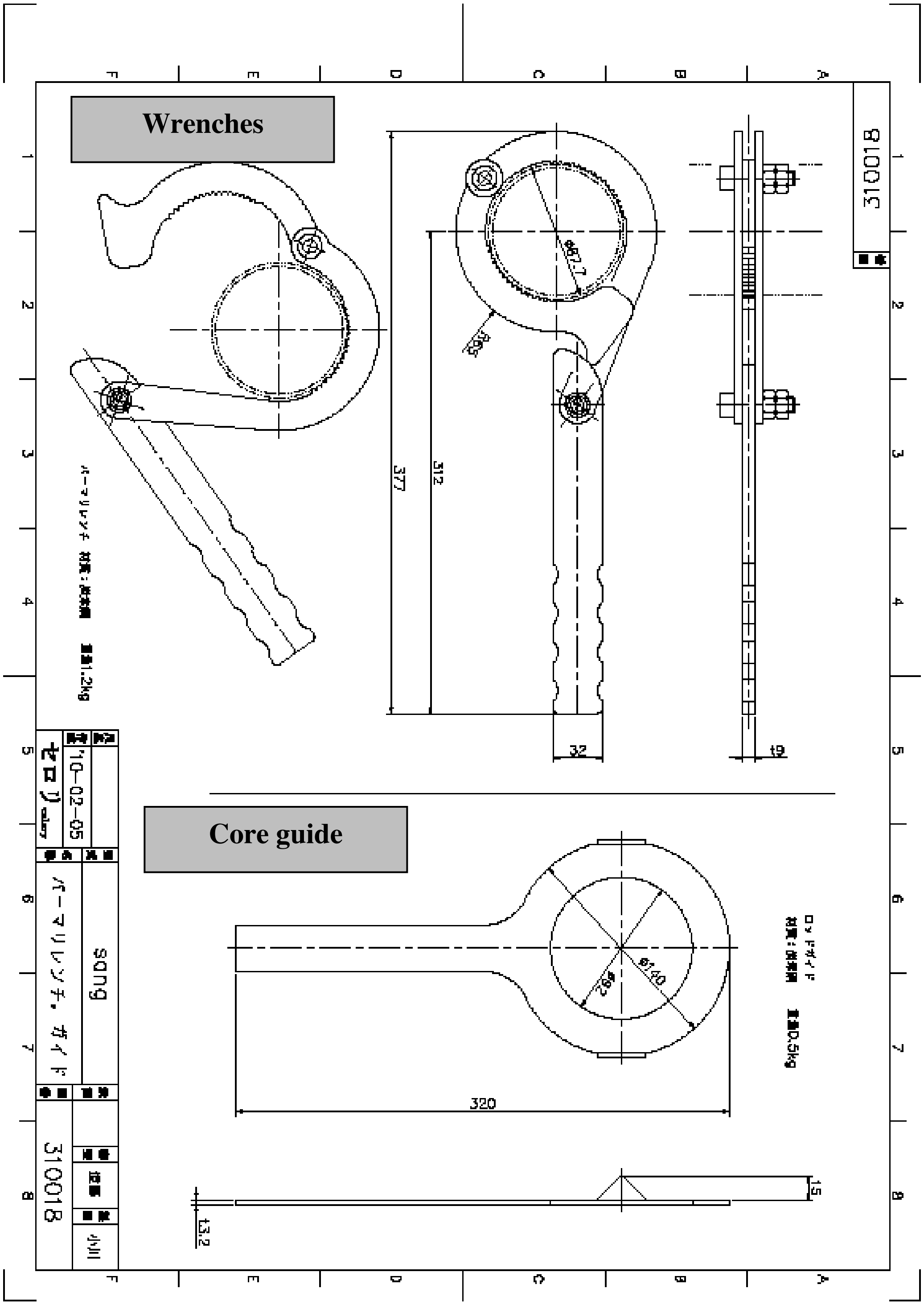

Figure 19 (c). Blueprint for the drill: wrenches and core guide.

3.3 Results

Our pneumatic drill for built by the engineer, Mr. Endo, worked outstandingly both on land and underwater. Table 5 shows the results of actual drilling underwater at both Gabgab Beach and Haputo Bay. The RPM on land without any extension tubes was 296, and the torque was 33.8 Newton-meters (Nm). It took 4 minutes to drill a 2.4 cm thick concrete block on land. For the actual sampling at the Gabgab coral site, it took 25 minutes to drill the 0.9 m coral core at a depth of 1.9 m, with no current. At Haputo Bay it took 80 minutes to drill the 0.88 m coral core at a depth of 7.2 m with a strong current. Figures 20 and 21 are the underwater drilling pictures at Haputo Bay and Gabgab Beach, respectively.

Table 5. Summary of drilling result

	Depth(m)	Time for drilling (minute)
2.4 cm thick cement	on land	4
0.9 m coral	1.9	25
0.88 m coral	7.2	80

Figure 20. Underwater drilling photo. The orange hose is sending the air from the compressor on the boat to the pneumatic drill. The blue hose is sending water from the pneumatic pump which provides continuous water flow to the drill bit to clean debris. The white hoses are the exhaust from the air motor.

Figure 21. The operation is simple and easy. No training is necessary. The drill goes down on its own, so the operator only needs to hold the drill. Extra pressure from the driller will speed up the drilling. Water gets cloudy from the drilling debris.

3.4 Discussion

There were three critical concerns about our new drilling system expressed by professionals experienced in both hydraulic and pneumatic methods: (1) in general pneumatic drills require RPM ranging from 800 to 1200, while ours was only 350 RPM (2) the bit and tube wall thickness is usually 2 mm while ours was 2.7 mm, which requires additional power to rotate, and (3) our system has no extra air supply system to clean the debris, which tends to accumulate at the bottom of coral samples while drilling. In addition to these concerns, one company specialized in underwater drilling suggested giving up on 80 mm cores and extracting 40 mm cores side by side, as they believed that pneumatic system was not adequate for 80 mm cores. All the concerns were carefully considered by our engineer. The key to solving all the challenges was to use a powerful air motor instead of the widely used pneumatic drill, and to use a gasoline-powered air compressor instead of scuba tanks.

The reason we had to spend double the expected amount of time to extract the core at Haputo Bay was originally thought to be due to the strong current and the depth which causes a loss of air pressure in the hose connecting to the air motor. However, it turned out upon subsequent inspection in the laboratory that the drilled specimen from Haputo Bay was unexpectedly hard. If this unexpected alteration was not the case, we believe that we could have drilled the specimen in much less than an hour. All in all, our method for underwater drilling proved to be a very simple, reliable, portable, and low-maintenance system. Our engineer is certain that we will be able to extract coral specimens up to 3 m simply by adding extensions. A remaining improvement for this methodology is adding a system to disburse or transport the debris away from the driller. The continuous debris cloud was bothersome during procedure, but deploying a waterproof fan or blower should take care of this problem.

4.0 Investigation of public SST datasets

4.1 Introduction

Instrumental SST data provides a means for calibrating and comparing the Sr/Ca proxy records from coral. Thus, obtaining reliable long-term instrumental SST data is one of the critical tasks for reconstructing coral records. Ideally, temperature loggers should be attached to corals at least for a year before drilling (Al-Rousan et al., 2003). However, this has not been widely done since most of the research facilities are remote from sample sites. Therefore, almost all the previous studies use a public SST dataset, gridded SST, or a locally available SST dataset instead of SST measured *in situ*. An important limitation of this approach is that there is a vast number of SST datasets created by models based on available instrumental data. In addition, there is usually no validation of a specific SST dataset selected for a given study. In the following section, we report on an inventory of existing SST datasets to identify the most reliable for coral-SST studies on Guam. It is important to know what datasets are available in the study area and how each available dataset is different from or consistent with others. One public dataset can be superior for certain regions, but inferior for other areas. It is essential to be aware of the limitations of public datasets, and to identify which is most suitable in the region of interest.

4.2 Methodology

From literature review (cf., Hurrel & Trenberth, 1999; Rayner et al., 2003; Reynolds & Smith, 1994), webpage research, and interviews with oceanographers and meteorologists, I identified 38 public SST datasets that cover the Western Pacific as shown in Table 7. It was very useful to use the dataset search tool provided by: (1) the International Research Institute for Climate and Society at Columbia University (IRI), and (2) the Computational and Information Systems Laboratory (CISL) at the National Center for Atmospheric Research (NCAR). Since SST datasets keep evolving from using different statistical techniques on existing datasets or combining two or more existing datasets, I often came across datasets that were already overtaken by a newer version and, thus no longer recommended for use. Those datasets were eliminated from the Table 7.

From Table 7, four major SST datasets were selected: (1) NOAA Extended SST v3b, (2) Hadley SST, (3) Reynolds and Smith olv1 and (4) Reynolds and Smith olv2. These were organized for the comparison to investigate how each dataset is different or similar for Guam (Figure 22). NOAA Extended SST v3b is gridded data for N14˚ × W144˚, and the other three datasets are for N13.5˚ × W144.5˚. I used MatLab software 2009 version b, from MathWorks for the data extraction of NOAA Extended SST v3b, ICOADS, and Reynolds and Smith olv1 and olv2. The syntax and coding for the data extractions are provided in Appendix.

As Reynolds and Smith olv1 and olv2 were calculated as sea surface temperature anomaly (SSTA), NOAA Extended SST v3b, ICOADS and Hadley SST data were converted into SSTA to calculate the correlation among these five datasets shown in Table 6. The time span for this calculation is from November 1981 to March 2003 as Reynolds and Smith olv1 was only available for this period.

4.3 Results

There were three types of SST measurement methods in the 38 datasets examined (Table 7): (1) satellite (2) *in situ* (buoy) and (3) ship. All the datasets are made from using one or more combinations of these methods. For the data processing, optimum interpolation (OI) and reduced space optimum interpolation (RSOI) seemed to be the popular statistical methods.

The correlations among four dataset are summarized in Table 6. The correlation varied moderately for the Guam region ($r = 0.79$ to $r = 0.99$). It is noteworthy that NOAA Extend SST v3b for N14˚ × W144˚ are correlating well with other three dataset for N13.5˚ × W144.5˚, and the 0.5˚ grid difference doesn't affect the SST trend for Guam. However, after 1998, Reynold & Smith olv.1 and Hadley SST started showing a large spread of about 0.5°C.

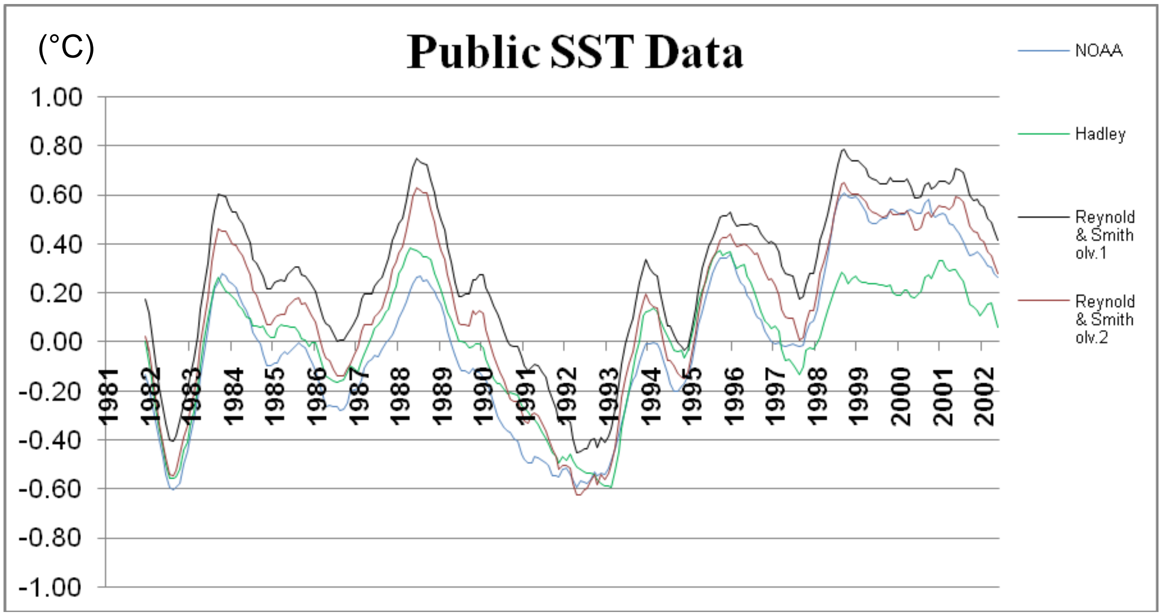

Figure 22. Comparison between the four public SST datasets for Guam. NOAA Extend SST v3 b (blue line), and Hadley SST (green line), Reynolds & Smith olv1 (black line) and Reynolds & Smith olv2 (brown line).

Table 6. Correlation among four public SST datasets based on the data from November 1981 to March 2003 for Guam

	NOAA	HADI	Reyn-Smith Olv1	Reyn-Smith Olv2
NOAA	-	-	-	-
HADI	0.787	-	-	-
Reyn-Smith Olv1	0.852	0.857	-	-
Reyn-Smith Olv2	0.872	0.875	0.987	-

Table 7. Inventory of public SST datasets which cover Guam

	Public Dataset	Type of Data	Data provider	Period	Resolution	Minimum Output	DATA Format
1	AVHRR Gridded 18km MCSST Level 3 (NAVOCEANO)	Satellite + Model	NASA	2001-2005	18km	weekly	FTP, POET, HEFT
2	AVHRR Oceans Pathfinder SST and buoy match-up data (Podesta et al.)	Satellite + Model	NASA	1985-Present	4km	daily	HTP, HEFT
3	AVHRR Orbital 9km MCSST Level 2 (NAVOCEANO)	Satellite + Model	NASA	1981-Present	9km	daily	FTP, NEREIDS, HEFT, OPeNDAP
4	AVHRR Pathfinder Global 9 km SST Climatology	Satellite + Model	NASA	1985-1999	9km	5day	FTP, HEFT
5	AVHRR Pathfinder SST v5	Satellite + Model	NASA	1981-2009	4km	daily	FTP, OPeNDAP,POET, HEFT
6	AVHRR weekly global 18km gridded MCSST (Miami)	Satellite + Model	NASA	1981-2001	18km	weekly	FTP, POET, HEFT, OPeNDAP
7	GFDL COADS Global Sea Surface Temperature Analyses, by Oort and Yi			1870 -1979			ASCII
8	GOES L3 6km Near Real-Time SST (NOAA/NESDIS)						
9	GOSTA atlas7 climatology	Ship+Satellite+Model	IRI	1951-1980	1X 1 and 5X5	monthly	
10	GOSTA atlas7 plus	Ship+Satellite+Model	IRI, BADC				HDF
11	GOSTA atlas8 climatology	Ship+Satellite+Model	IRI				
12	GOSTA atlas8 plus	Ship+Satellite+Model	IRI, BADC	1856-1995			HDF
13	HadISST1 (Former GISST)	Ship+Satellite+Model	MetOffice	1871-Present	1X1	monthly	gz
14	HadSST2 (Former MOHSST)	Ship+Satellite+Model	MetOffice	1850-Present	5X5		gz
15	Hansen's NODC EPOCS Drifting Buoy Observations	Buoy +Satellite+Model	NODC	1974-1984		6 hour	
16	ICOADS	Ship+Satellite+Model	NOAA	1960-present	1X 1 and 2X2	monthly	CV, net CDF
17	IGOSS nmc Reyn_SmithOIv1 monthly ssta	Ship + Buoy + Satellite +Model					
18	IGOSS nmc Reyn_SmithOIv2 monthly ssta	In situ + Sattelite+Model					
19	Japanese 25-year Reanalysis Project	In situ +Satellite+Model	JMA	1974-2004	1.125X1.121	6hour	WMO GRIB
20	Japanese 25-year Reanalysis Project, Monthly Means	In situ +Satellite+Model	CISL	1979-2008	1.125X1.121	6hour	netCDF
21	MODIS Aqua Global Level 3 Mapped Mid-IR SST						
22	MODIS Aqua Global Level 3 Mapped Thermal IR SST						
23	MODIS Terra Global Level 3 Mapped mid-IR SST						
24	MODIS Terra Global Level 3 Mapped Thermal IR SST						
25	NAVOCEANO MCSST Level 2 HRPT/LAC Data						
26	NCEP Reynolds Historical Reconstructed Sea Surface Temperature Data Set						
27	NCEP Reynolds Optimally Interpolated Sea Surface Temperature Data Sets						
28	NCEP Version 2.0 OI Global SST	In situ +Ship+Satellite+Model	NCAR	1981-Present	1X1		
29	NOAA Extended Reconstructed Sea Surface Temperature (SST) V3b			1854 – 2010	2 X 2	monthly	netCDF
30	NOAA NCEP EMC CMB GLOBAL Reyn_SmithOIv1 monthly ssta	Ship + Buoy + Satellite+Model					
31	NOAA NCEP EMC CMB GLOBAL Reyn_SmithOIv2 monthly ssta	In situ + Satellite + SSTs simulated by sea ice cover+Model	IRI	1960-2010	1X1	monthly	
32	NOAA NODC WOA01	In situ + Model	IRI		1X1 and 5x5	monthly	ASCII
33	NOAA Optimum Interpolation 1/4 Degree Daily SSTA Version 2	Ship + Buoy + Satellite+Model	NOAA	1981-Present	0.25X0.25		netCDF
34	NSIPP AVHRR Pathfinder and Erosion Global 9km SST Climatology (Casey, Cornillon)						
35	Ocean Circulation & Currents Product: global 0.5 and 1.0 deg grids (JPL, WOCE v3)						
36	Pacific Sea Surface Temperature and Wind Analyses, by Rasmussen and Carpenter			1946-1976	2 X 2	monthly	ASCII
37	Shea and Trenberth's Global Monthly Sea Surface Temperature Climatology			1950-1979	2X2	monthly	ASCII
38	U.K. Sea Surface Temperature Analyses		MetOffice	1854-1968	5X5	monthly	WMO GRIB

4.4 Discussion

The aforementioned inconsistencies between public datasets and the data reported by different techniques reflect observations reported by others. Chan and Gao (2005), for example, reported large discrepancies (0.5ºC to 1ºC) between the results from the MODIS (Moderate resolution imaging spectroradiometer), NCEP (National Center for Environment Protection) and TMI (Tropical Rainfall Measuring Mission Microwave Imager) in the tropical Atlantic, tropic western Pacific, Bay of Bengal, and the Arabian Sea. Hurrel and Trenberth (1999) reported a large difference of ~2ºC in higher latitudes between Reynolds and Smith's SST and GISST. Also they stated that correlations between four datasets: two different statistical methods from NCEP, Global Sea-Ice and SST (GISST) are less than r = 0.75 in tropical pacific. Therefore, one should be aware of these differences, and cautious when identifying the most suitable dataset for a given study region and purpose. The errors in SST in the tropics can affect predictions of moist convection, and other components of the hydrological cycle by general circulation models (Hurrel et al., 2008).

5.0 Geochemical analysis of corals

5.1 Introduction

Coral $\delta^{18}O$ is used as a geochemical proxy to reconstruct past SST and sea surface salinity (SSS). The analysis based on coral $\delta^{18}O$ was started in the 1970's. Weber and Woodhead (1972) originally discovered the correlation between coral $\delta^{18}O$ and SST. Later on they discovered Sr/Ca coral can also be used as proxy for past SST reconstruction (Weber, 1973). Until the 1990's, most researchers used only coral $\delta^{18}O$ for both past SST and SSS reconstruction. After high-precision thermal ionization mass spectrometry (TIMS) emerged in 1992 and became widely available, researchers started using both coral $\delta^{18}O$ and Sr/Ca coral for SST reconstruction. According to Gagan et al. (2000), TIMS has a precision of 0.03 %, and can thus distinguish temperature increments of 0.05˚C. Currently this SST-coral Sr/Ca linear relationship is widely known and, according to Correge (2006), 19 out of 33 studies showed the correlation higher than R^2 = 0.7. The intercepts of the regression lines for SST (X axis) and coral Sr/Ca (Y axis) are between 10.073 and 11.12 among these 19 studies. Also, this relationship has been demonstrated in controlled laboratory experiments (cf., Smith et al., 1979, Reynaud et al., 2004).

In our study, we analyzed coral Sr/Ca from Gabgab Beach. There are four reasons for choosing Sr/Ca instead of coral $\delta^{18}O$: (1) Gegan et al. (2000) noted that coral Sr/Ca-SST relations have been published for only nine sites in Pacific and Indian Oceans: New Caledonia, Hawaii, two sites in Taiwan, three sites in Australia, Indonesia and Papua New Guinea. They concluded that the linear relationships from these sites were remarkably similar, and it is very significant to add Guam data from the western Pacific to these nine sites. (2) Asami et al. (2005) reported that coral $\delta^{18}O$ in Guam is influenced by both SST and SSS. Since the focus of our project was SST, we chose to focus on Sr/Ca at this point, as it is a less equivocal proxy of SST, assuming that it is less sensitive to SSS than $\delta^{18}O$. (3) Correge (2006) advised that this type of research should examine the possibilities of environmental and biological factors, such as water chemistry, that can affect coral calcification. We assumed coral Sr/Ca has less sensitivity than $\delta^{18}O$ to be influenced by environmental factors as Sr/Ca of seawater is believed to be steady. Sr/Ca seaward for modern oligotrophic reef settings ranges from 8.51 to 8.55 mmol/mol (Gagan et al., 2000). As mentioned in section 2.2.1.1, we collected Sr/Ca of seawater to verify this common assumption, and (4) the sample in this project is from Gabgab Beach which is only ~90 m away from the shore. This situation raised the possibility that seawater $\delta^{18}O$ may vary due to freshwater discharge at this location. For these four reasons, we chose and expected Sr/Ca coral to be a better proxy, more than $\delta^{18}O$ coral, for the SST investigation in this study.

5.2 Methodology

The permit for our sampling was issued by the Guam government Department of Agriculture, license number 10-013. In July 2010, a coral core, 94 cm long and 80 mm in diameter was collected using the a custom pneumatic drill, summarized in section 3.0 and described in detail by Bell et al., 2011, at ~90 m seaward from Gabgab Beach. In August 2011, a 90 cm long and 80 mm in diameter core was collected ~200 m seaward from the shore in Haputo Bay using the same drill (Figure 1). The coral cores were drilled parallel to the growth axis from dosal (live polyp part) to basal (sediment part). The species was identified as *Porites lutea* at the Marine Laboratory at the University of Guam. In the laboratory at UTA, the sample from Gabgab Beach was slabbed to 12 mm. This is thicker than general methodology, but this thickness was chosen as the sample would have to handle the trip back to Guam. X-radiograph images were taken to identify the growth axis. Unfortunately it was not feasible to make slabs from the coral samples at Haputo Bay due to heavy alteration.

The slabs were washed by an ultrasonic cleaner for 60 minutes on each side of the slabs. Then the slabs were dried in an oven overnight. After the slabs were clean and dry, 5 mm wide tape was placed on the slabs along the sample growth axis to guide the drilling process. As the annual band was about 1.5 cm, we decided to prepare the samples every 1.2 mm, the average monthly growth, to obtain approximately monthly SST resolution. A total of 616 samples were prepared by computer controlled Micro-Mill (Figure 23), and each sample was 1.2 mm wide by 0.05 mm deep. These 616 samples were weighed and digested with 2% HCl, and Sr/Ca coral analysis was conducted by ICP-OES.

To convert the values of Sr/Ca coral to time series values, the method suggested by the laboratory at UTA was applied. This procedure is similar to that of Asami et al. (2005). First, the spreadsheet column for the time series was made right next to the Sr/Ca values in the spreadsheet. The highest Sr/Ca values were checked within 10 to 15 cells and grouped as one year growth, since the annual band is about 1.5 cm and the sample was prepared every 1.2 mm. In general, February has the lowest SST on the island. Thus, the highest Sr/Ca value in each annual group was assigned to February. After that, for each Sr/Ca value, the date was interpolated and assigned. Then Sr/Ca data spanning each year were interpolated into 12 (monthly) values for the respective year. This Sr/Ca plot was then compared to the Hadley SST (Figure 24) because it showed the best match with the UOG logger attached to the coral sample, as discussed in section 2.2.1.1.

In addition to the comparison to SST, which is a general protocol in this type of study, we compared this Sr/Ca value to four meteorological factors relevant to Guam and the Western Pacific: (1) maximum air temperature from AAFB (2) sea level from Apra Harbor tide gage, and (3) the ENSO index from NASA (http://www.esrl.noaa.gov/psd

/data/correlation/censo.data). (4) local precipitation from Andersen Air Force Base (AAFB). Also, we pooled the data from July to September which are from the wet season segment of the coral core, and from December to March, which are from the dry season segment of the coral core to see how these two types of bands corresponds to the SST-Sr/Ca relationship.

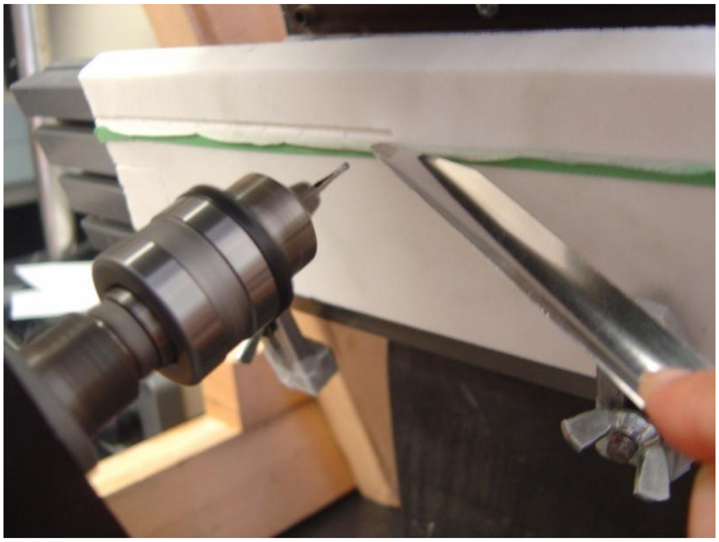

Figure 23. The procedure to prepare 616 samples by computer controlled Micro-Mill.

5.3 Results

5.3.1 Coral Sr/Ca vs Hadley SST

Figure 24 shows coral Sr/Ca and Hadley SST from 1960. Hadley SST shows a 0.5°C increase for the past 140 years around Guam. From 1960 to 2010, this dataset is showing the similar general long term linear trend and annual pattern as the coral Sr/Ca. Over all, the correlation between these two curves was high (r= -0.74). We also calculated the correlation between coral Sr/Ca anomaly and SST anomaly to see if they can still respond each other without annual cycle influence. The correlation was still confirmed (r= 0.47). However, although there is a clear one-to-one correspondence in the seasonal cycles, the Sr/Ca and Hadley SST do not show a consistent phase relationship. Therefore, further analysis was needed to investigate this coral Sr/Ca-SST relationship.

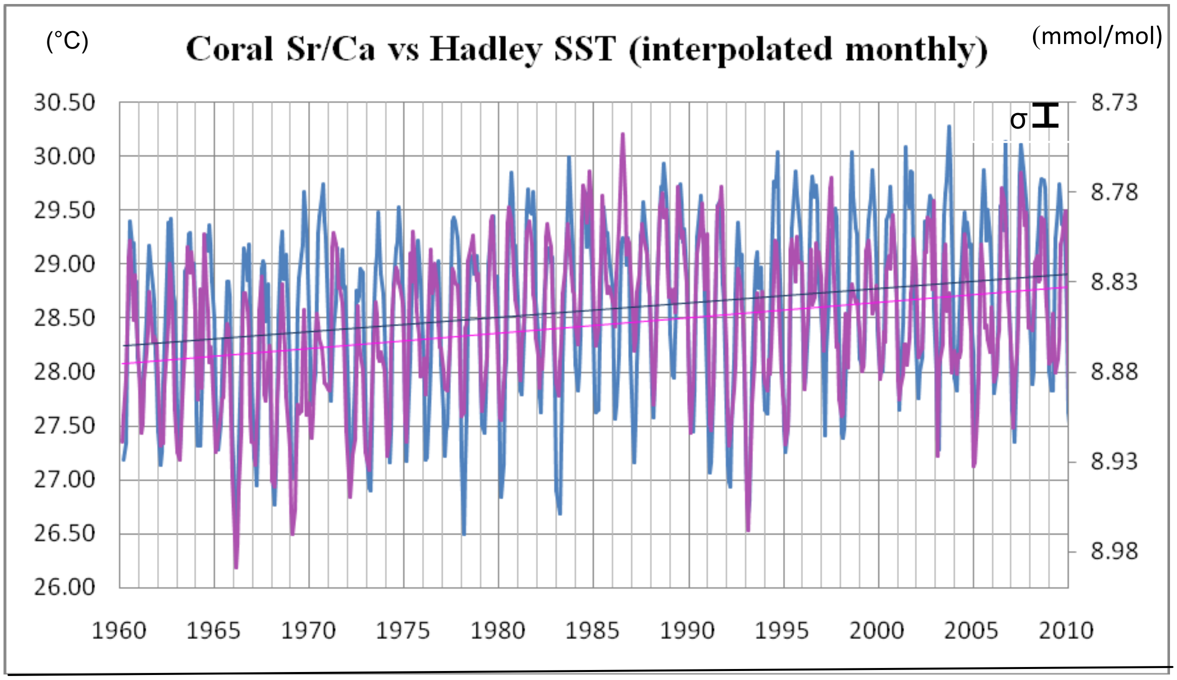

Figure 24. Comparison between Hadley SST data (˚C) (blue line) and coral Sr/Ca (mmol/mol) (pinkline). Linear lines are showing long term trend for each dataset.

5.3.2 Coral Sr/Ca vs maximum air temperature, sea level, ENSO index and precipitation

We plotted coral Sr/Ca against maximum air temperature, sea level and ENSO index respectively (Figure 25). We took a 12-month average for this figure. Only coral Sr/Ca and maximum air temperature shows a similar trend among these three (r = 0.492). With respect to sea level and ENSO index, we didn't see similar trends, and we didn't find specific regularity in these three figures. The correlation between each metrological factor and coral Sr/Ca is summarized in Table 7. Maximum air temperature and Hadley SST dataset showed a moderate correlation of r = 0.628. Also, sea level and ENSO index showed a weak correlation r = -0.534.

Table 7. Correlation (r) between five metrological factors and coral Sr/Ca on Guam.

	Air Temperature	Sea Level	ENSO Index	Precipitation	Hadley SST
Air Temperature	-	-	-	-	-
Sea Level	0.353	-	-	-	-
ENSO Index	0.004	-0.534	-	-	-
Precipitation	0.052	0.477	-0.053	-	-
Hadley SST	0.628	0.474	-0.113	0.455	-
Coral Sr/Ca	-0.492	-0.29	0.083	-0.38	-0.741

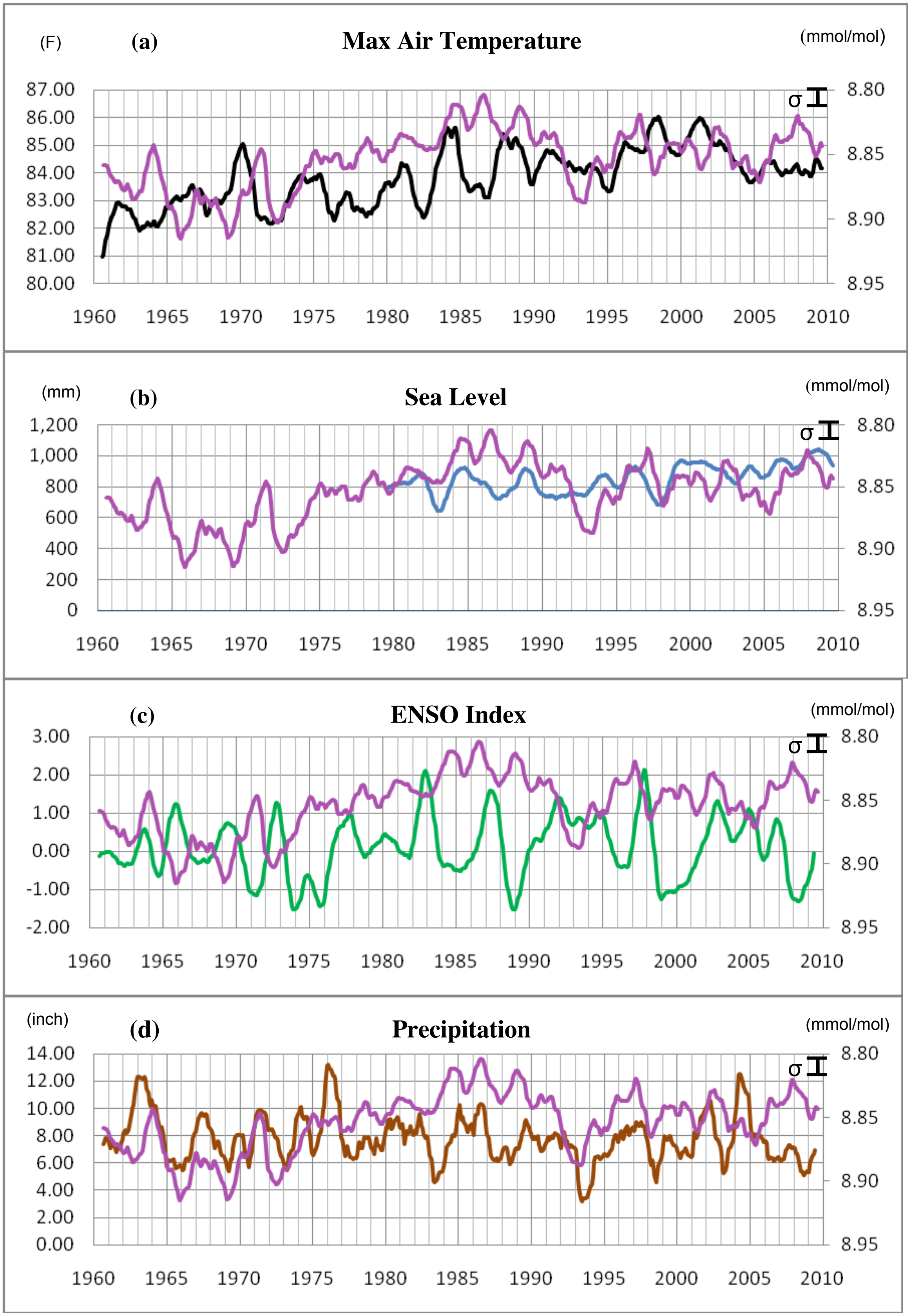
(F)
(a)
Max Air Temperature
(mmol/mol)
87.00
86.00
85.00
84.00
83.00
82.00
81.00
80.00
σ
8.80
8.85
8.90
8.95
1960 1965 1970 1975 1980 1985 1990 1995 2000 2005 2010
(mm)
(b)
Sea Level
(mmol/mol)
1,200
1,000
800
600
400
200
0
σ
8.80
8.85
8.90
8.95
1960 1965 1970 1975 1980 1985 1990 1995 2000 2005 2010
(c)
ENSO Index
(mmol/mol)
3.00
2.00
1.00
0.00
-1.00
-2.00
σ
8.80
8.85
8.90
8.95
1960 1965 1970 1975 1980 1985 1990 1995 2000 2005 2010
(inch)
(d)
Precipitation
(mmol/mol)
14.00
12.00
10.00
8.00
6.00
4.00
2.00
0.00
σ
8.80
8.85
8.90
8.95
1960 1965 1970 1975 1980 1985 1990 1995 2000 2005 2010

Figure 25. Comparison between coral Sr/Ca (mmol/mol) (pink line) and (a) max air temperature, Andersen AFB (F) (black line); (b) sea level, Apra Harbor (inches) (blue line); (c) NASA ENSO index (green line); (d) precipitation, Andersen AFB (inches) (brown line) based on 12 month running average.

5.3.3 Coral wet season/long daylight/higher SST segment *vs* dry season/short daylight/lower SST segment

It has long been noted by coral specialists that coral banding reflects differences in seasonal growth rates, usually manifest as light-colored bands that reflect the faster growth during higher SST months (wet season), and dark color bands reflecting slower growth during lower SST months (dry season) (Lough and Barnes, 1989). Identifying such banding precisely was beyond the scope of this study. We undertook a first-order analysis of the seasonal relationship by constructing separate curves for each assumed season: one from higher SST months, June to September, representative of the wet season and one from December to March, representative of the dry season. The wet-season curve (Figure 26-a), showed much lower correlation with the Hadley SST (r = 0.37) compared to the pooled data from December to March (r=0.64) (Figure 26-b). The intercepts of the regression lines for the SST (X axis) and the coral Sr/Ca (Y axis) from wet season is 9.68 and the one from dry season is 10.05 (Figure 27).This result from wet season is not close to any of the studies reviewed in Correge (2006). On the other hand, the result from dry season, y = -0.041x+ 10.05, and from all the data, y = -0.037x + 9.92, is similar to the study from New Caledonia (Correge, 2006), y = -0.039x + 9.95 (Figure 27). It is thus inferred that additional factors related to wet season, make the relationship between SST and coral Sr/Ca more complicated during the wet season than during the dry season. It is noteworthy that based on Hadley SST data from January 1960 to January 2010, average from July to September SST is 29.3 °C while the one from December to March is 27.7 °C. Thus, the higher temperature or precipitation during wet season may be one of the stress factors for the coral Sr/Ca-SST relationship at Gabgab Beach.

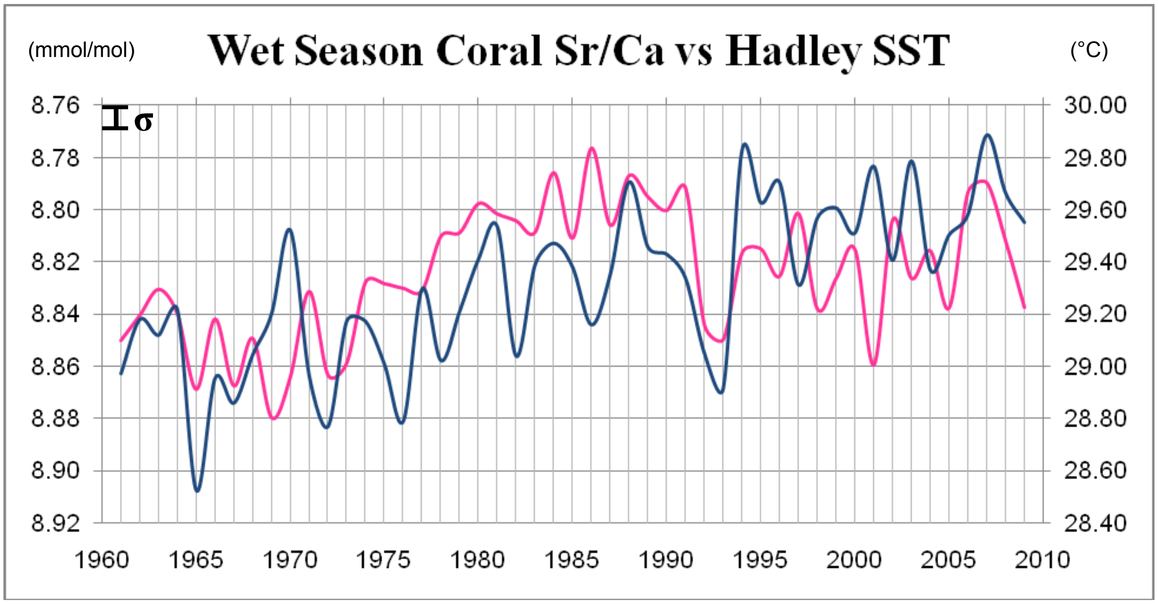

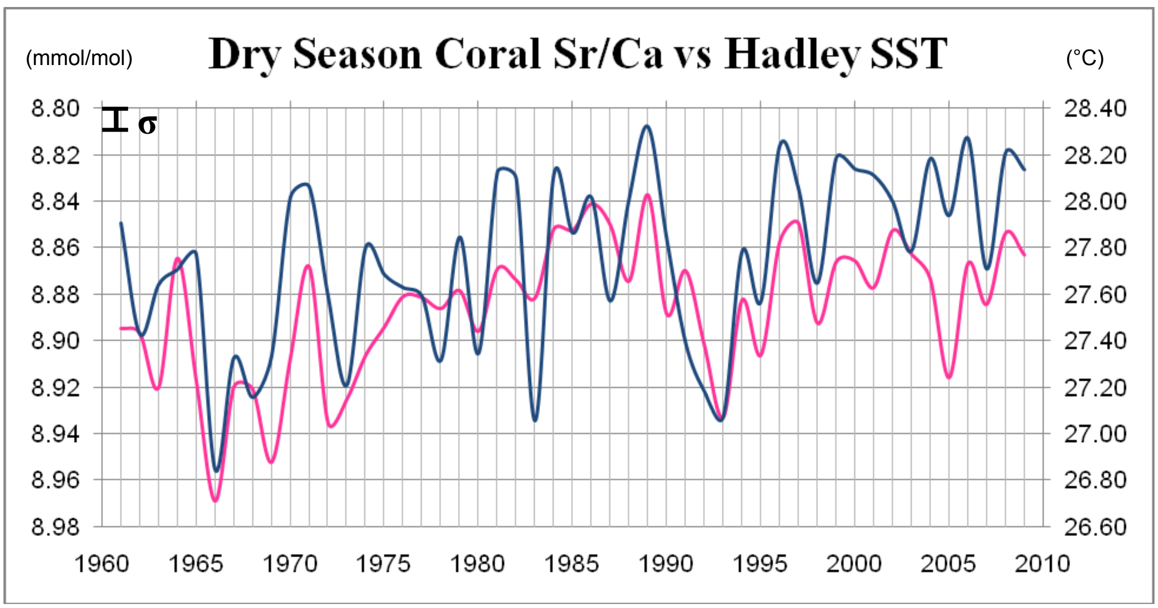

Figure 26 (a). The pooled data from higher SST months, from July to September (wet season). **(b)**.The pooled data from lower SST months, from December to March (dry season), Sr/Ca (mmol/mol) (pink line) and Hadley SST (°C) (blue line).

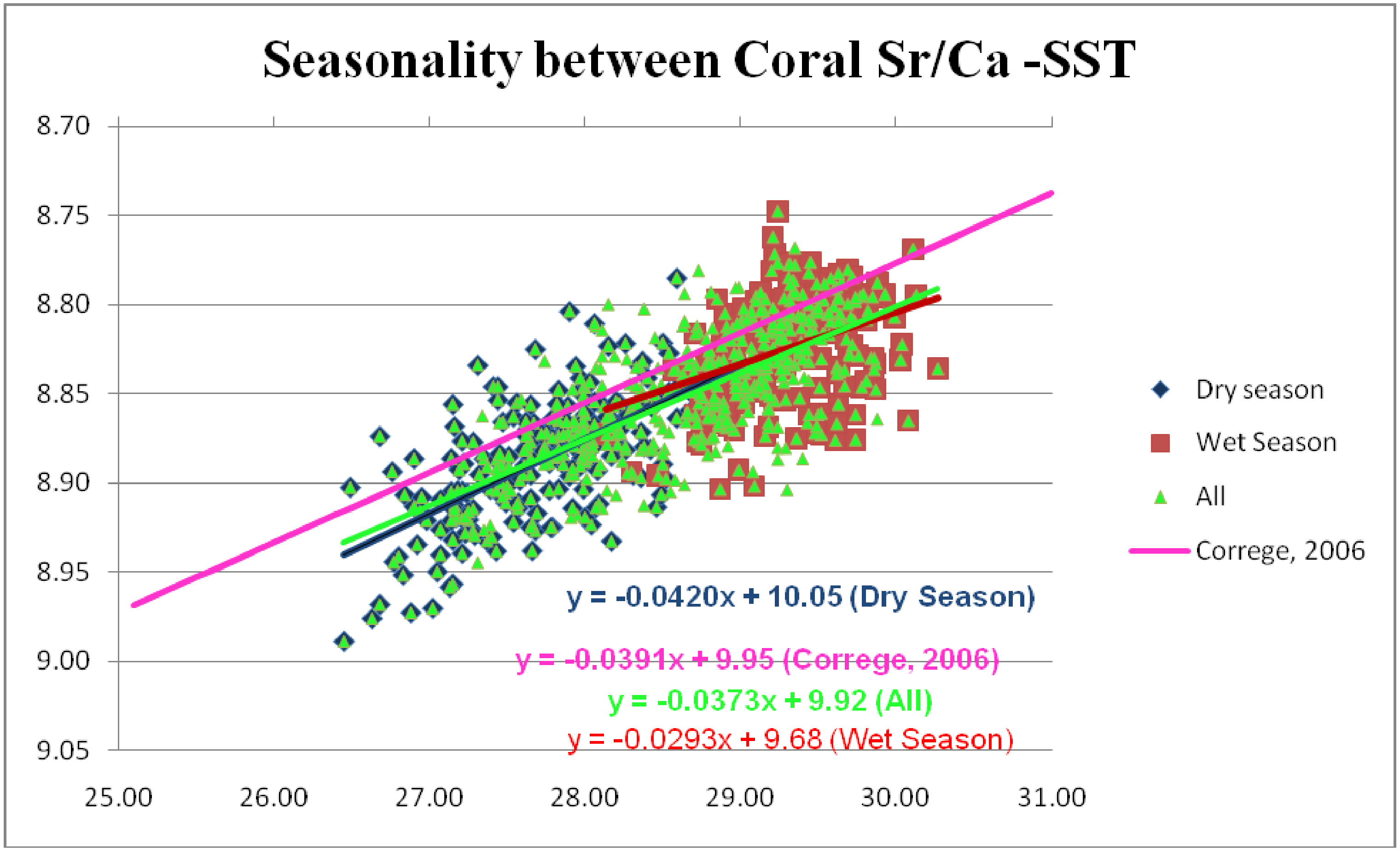

Figure 27. Seasonality in linear relationship between Coral Sr/Ca and Hadley SST. The pooled data from dry season segment (blue), the pooled data from wet season segment (red), all the data (green). The pink regression line is from Correge, 2006.

5.4 Discussion

The coral Sr/Ca at Gabgab Beach is correlating well with the Hadley SST, which is showing a 0.5˚C increase for the past 140 years. This upward trend in SST is consistent with the fact that sea level is rapidly rising in Guam (about 20 cm for the past 30 years from the figure 25-b). According to the European Environment Agency (2010), global mean sea surface temperature is 1.0˚C higher than 140 years ago, although the sea surface temperature change around Guam appears to not be as rapid as in other areas. However, our coral sample appears to be affected by some factors related to wet season, and further investigation of the coral physiology will be needed to identify the stress factors which cause this failure to exhibit coral Sr/Ca and SST relationship.

There are at least three hypotheses for what the corals at Gabgab Beach are experiencing during wet season: (1) the chemistry of seawater that goes to coral membranes is changing and (2) the Sr/Ca pump at coral membranes is functioning differently due to higher SST or (3) higher pH in inner coral calcifying fluids. Regarding first assumptions, our time series Sr/Ca seawater analysis is underway, and the result from this analysis will be able to evaluate this assumption. It is noteworthy that Ferrier-Pagès et al. (2002) demonstrated that the concentration of Sr in seawater did not affect the coral Sr/Ca. Thus, he believes that kinetics is more influential to coral Sr/Ca than seawater chemistry. For the second and third hypotheses, Allison (2010) conducted an experiment which shut down the enzyme CaATPase, a carrier that transports Ca in seawater to coral for calcification process, and concluded that shutting it down didn't change coral Sr/Ca. Thus, there is a possibility that the enzyme responsible for Sr path is functioning differently due to some stress factors related to wet season on Guam. For instance, SST during June to September may not be ideal for the enzyme to transport Sr from seawater to coral. According to Cohen (2001), photosynthesis activity changes the pH level in calcifying fluids in corals as carbon dioxide will be actively removed by algae cell, zooxanthellate. It is apparent that June to September tend to receive more radiation, thus causing higher photosynthesis activity which increases pH level in inner coral calcifying fluids. As of now, it is unknown which enzyme is responsible for Sr processing which should be playing a key role for Sr/Ca kinetic and being controlled by SST and pH fluctuations, so it is not feasible to conduct a laboratory experiment yet. Identifying this enzyme and investigating its function will be the first step to reveal Sr role in the coral calcification system.

6.0 Conclusion and recommendation for further study

From this project, we could confirm the significance of investigation around the samples for climate reconstruction. It is the knowledge of hydrology and water analysis at sample sites that will help us identify the best samples for further analysis to investigate past SST and precipitation. From this study, we could identify and group three types of conceptual pathways on the island (Figure 28): the first path is the SST at the Gabgab Beach coral site, Hadley public SST dataset, coral Sr/Ca, and local precipitation (especially dry and wet peak history). The second path is the SST at the Gabgab Beach coral site, Hadley public SST dataset, the $\delta^{18}O$ seawater at Gabgab Beach, $\delta^{18}O$ rainwater from UOG station, local precipitation from six sites and $\delta^{18}O$ dripwater at stumpy and station 1. The third path is the relationship between $\delta^{18}O$ dripwater and $\delta^{18}O$ stalagmite at stumpy and station 1. Partin et al. (submitted) revealed that the combination of Mg/Ca and $\delta^{18}O$ stalagmite from Stumpy may reveal the decadal scale of drought history. It is still unknown whether Stumpy or other stalagmites can resolve yearly changes in drought history. Further analysis of the stalagmites will provide useful and productive comparison to corals. Also, if we can analyze more corals from Gabgab Beach which have longer records than that used in this study, it will allow us to compare these two valuable climate proxies that are already proven to have significant climate records.

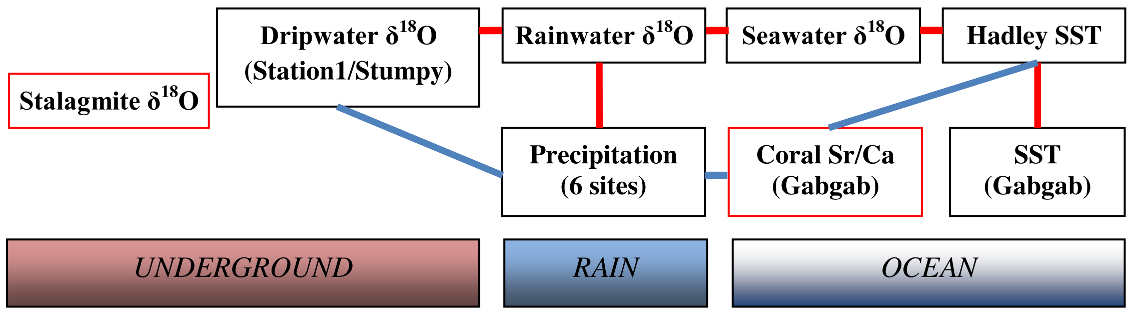

Figure 28. Hydrologic cycle for climate study based on *in situ* monitoring and geochemical analysis in Guam. Black boxes show factors for in situ monitoring. Red boxes indicate geochemical analysis. Red line between boxes show confirmed strong correlations and blue line show confirmed moderate correlations.

References

Adachi, H., & Abe, O. (2003). "Air drill" for submerged massive coral drilling. *Marine Technology Society Journal,* 37(2), 31-36.

Al-Rousan, S., Al-Moghrabi, S., Patzold, J., & Wefer, G. (2003). Stable oxygen isotopes in Porites corals monitor weekly temperature variations in the northern Gulf of Aqaba, Red Sea. *Coral Reefs*, 22, 346-356.

Allison, N., Cohen, I., Finch, A., & Erez, J. (2010). Controls on Sr/Ca in Scleractinian Corals: The effects of Ca-ATPase and Ca channels on skeletal chemistry. American Geophysical Union, Fall Meeting 2010, abstract #PP21D-08.

Asami, R., Yamada, T., Iryu, Y, Quinn, T. M., Meyer, C. P., & Paulay, G. (2005). Interannual and decadal variability of the western Pacific sea surface condition for the years 1787-2000: Reconstruction based on stable isotope record from a Guam coral. *Journal of Geophysical Research*, 110, C05018.

Bell, T., Endo, T., Jenson, W. J, Bell, F. R., Lander, A. M. (2011). Pneumatic underwater drill for extracting coral cores. *WERI Technical Report*, 135.

Betancourt, J. L., Grissino-Mayer, H. D., Salzer, M. W., & Swetnam, T. W. (2002). A test of "annual resolution" in stalagmites using tree rings. *Quaternary Research*, 58, 197-199.

Carlucci, A. F., & Strickland, J. D. H. (1968). The isolation, purification and some kinetic studies of marine nitrifying bacteria. *Journal of Experimental Marine Biology and Ecology*, 2(2), 156-166.

Chan, P. K., & Gao, B. C. (2005). A comparison of MODIS, NCEP, and TMI sea surface temperature datasets. *Geoscience and Remote Sensing Letters*, 2(3), 270-274.

Charles, C., Lynch-Stieglitz J., Ninnemann U. S., & Fairbanks, R. G. (1996). Climate connections between the hemispheres revealed by deep sea sediment core/ice core correlations. *Earth Planetary Science Letter*, 142 (1), 19-27.

Cohen, A. L, Owens, K. E., Layne, D. G., & Shimizu, N. (2002). The Effect of Algal Symbionts on the Accuracy of Sr/Ca Paleotemperatures from Coral. *Science*, 296, 331-333.

Cook, E. R. (1995). Temperature histories from tree rings and corals. *Climate Dynamics*, 11(4), 211-212.

Correge, T. (2006). Sea surface temperature and salinity reconstruction from coral geochemical tracers. *Paleoceanography, Paleoclimatology, Paleoecology*, 232, 408-428.

Crowley, T. J. (2000). CLIMAP SSTs re-revisited. Climate Dynamics, 16:241-255.

Cruz Jr, F. W., Karmann, I., Viana Jr, O, Burns, S. J., & Ferrari, J. A. (2005). Stable isotope study of cave percolation waters in subtropical Brazil: Implications for paleoclimate inferences from speleothems. *Chemical Geology*, 220, 245-262.

Dansgaard, W. (1964). Stable isotopes in precipitation. *Tellus*, 16(4), 436-468.

Easton, W. H. (1981). A submersible, rechargeable, electric drill. *Atoll Research Bulletin,* 255: 83-90.

European Environmental Agency. (2010). Rising sea surface temperature: towards ice-free Arctic summers and a changing marine food chain. Retrieved March 30, 2011 from http://www.eea.europa.eu/themes/coast_sea/sea-surface-temperature

Ferrier-Pagès, C., Boisson, F., Allemand, D., & Tambutté, E. (2002). Kinetics of strontium uptake in the scleractinian coral *Stylophora pistillata*. *Marine Ecology Progress Series,* 245, 93-100.
Gagan, M. K., Ayliffe, L. K., Beck, J. W., Cole, J. E., Druffel, E. R. M., & Dunbar, R. B. et al. (2000). New views of tropical paleoclimates from corals. *Quaternary Science Reviews*, 19, 45-64.
Genty, D., Baker, A., & Vokal, B. (2001). Intra- and inter-annual growth rate of modern stalagmites. *Chemical Geology*, 176 (1-4), 191-212.
Hill, C. A. (1999). Mineralogy of Kartchaner caverns, Arizona. *Journal of Cave and Karst Studies, 61*(2), 73-78.
Hurrel, J. W., Hack, J. J., Shea, D., Caron, J. M., & Rosinski, J. (2008). A new surface temperature and sea ice boundary dataset for the community atmosphere model. *American Meteorological Society*, 5145-5153.
Hurrel, J. W., & Trenberth, K. E. (1999). Global sea surface temperature analyses: Multiple problems and their implications for climate analysis, modeling and reanalysis. *Bulletin of the American Meteorological Society*, 12(80), 2661-2678.
Isdale , P., & Daniel, E. (1989). The design and deployment of a lightweight submarine fixed drilling system for the acquisition of coral cores. *Marine Technology Society Journals,* 23, 3-8.
Jiménez-Sánchez, M., Stoll, H., Vadillo, I., López-Chicano, M., Domínguez-Cuesta, M., Martín-Rosales, W., et al. (2008). Groundwater contamination in caves: four case studies in Spain. *International Journal of Speleology*. 37(1), 53-56.
Lough, J. M. & Barnes, D. J. (1989). Intra-annual timing of density band formation of Porites coral from the central Great Barrier Reef. *Journal of Experimental Marine Biology and Ecology*. 135(1), 35-57.
Kan, H., Adachi, H., Nakajima, H., & Naito, G. (1998). Development of submersible, diver operating coring device. *Chishitsu New*s, 527, 43-47.
Kester, D. R., Duedall, I. W., Connors, D. N., & Pytkowicz, R. M. (1967). Preparation of artificial seawater. *Limnology and oceanography*, 12(1), 176-179.
Li, B., Nychka, D. W., & Ammann, C. M. (2010). Value of Muti-proxy Reconstruction of Past Climate. *Journal of the American Statistical Association,* 105(491), 883-895.
McDermott, F., Mattery, D. P., & Hawkesworth, C. (2001). Centennial-scale Holocene climate variability revealed by a high-resolution speleothem δ18O record from SW Ireland. *Science*, 294, 1328-1330.
Marubini, F., & Davies, P. S. (1996). Nitrate increases zooxanthellae population density and reduces skeletogenesis in corals. *Marine Biology*, 127, 319-328.
NASA. (2009). Global Seawater Oxygen-18 Database. Retrieved June 9, 2009, from http:// data.giss.nasa.gov/o18data/
Neukom, R., Luterbacher, J., Villalbra, R., Kuttel, M., Frank, D. et al. (2010). Multiproxy summer and winter surface air temperature field reconstructions for southern South America covering the past centuries. *Climate Dynamics*, DOI 10.1007/s00382-010-0793-3
Partin, J. W., Cobb, K. M., Adkins, F. J., Clark, B., & Fernandez, P. D. (2007). Millennial-scale trends in west Pacific warm pool hydrology since the Last Glacial Maximum. *Nature*, 449, 452-455.

Partin, J. W., Jenson, J. W., Banner, J. L, Terrence, Quinn, M., Taylor, F. W., Sinclair, D. et al. (submitted). Modern relationship between rainfall variability, cave dripwater and stalagmite geochemistry in Guam, USA.

Quinn, T. M., Taylor, F. W., & Crowley, T. J. (2006). Coral-based climate variability in the Western Pacific Warm Pool since 1867. *Journal of Geophysical Ressearch*, 111, C11006.

Reynaud, S., Ferrier-Pagès, C., Boisson, Florence, Allemand, D., & Fairbanks, R. G. (2004). Effect of light and temperature on calcificationand strontium uptake in the scleractinian coral *Acropora verweyi*. Marine Echology Progress Series, 279, 105-112.

Rayner, N. A., Parker, D. E., Horton, E. B., Folland, C. K., Alexander, L. V. et al. (2003). Global analysis of sea surface temperature, sea ice, and night marine air temperature since the late nineteenth century. *Journal of Geophysical Research*, 108(2), 1-22.

Reynolds, R. W., & Smith, T. M. (1994). Improved global sea surface temperature analyses using optimum interpolation. *Journal of Climate*, 7, 929-948.

Rohling, E. J. (2007). Oxygen isotopic composition of seawater. *Paleoceanography physical and chemical proxies/Oxygen isotopic composition*, 1748-1756.

Smith, S. V., Buddemeier, R. W., Redalje, R.C., & Houck, J. E. (1979). Strontium-calcium thermometry in coral skeletons. *Science* (204), 404-407.

Wafar, M. (1990). Nitrification in reef corals. *Limnology and oceanography*, 35(3), 725-730.

Weber, J. N. (1973). Incorporation of strontium into reef coral skeletal carbonate. *Geochimica Cosmochimica Acta*, 37, 2173–2190.

Weber, J. N. , & Woodhead, P. M. J., (1972). Temperature dependence of oxygen-18 concentration in reef coral carbonates. *Journal of Geophysical Research*, 77, 463-473.

Yap, C. K., Ismail, A., Misri, K., & Tan, S. G. (2005). Nitrate concentrations in the surface seawater of the straits of Malacca. *Asian Journal of Water, Environment and Pollution*, 2, 45-49.

A. MatLab code and syntax to retrieve the public SST dataset.

Step1. Open the file

sst=[];	**sst**
sst=netcdf.open('sst.mnmean.nc','NC_NOWRITE');	**sst3**
[ndims,nvars,ngatts,unlimdimid] = netcdf.inq(sst)	**ndims,nvars,ngatts,unlimdimid**
[varname,xtype,dimids,natts] = netcdf.inqVar(sst,0)	**varname lat**
[varname,xtype,dimids,natts] = netcdf.inqVar(sst,1)	**varname lon**
[varname,xtype,dimids,natts] = netcdf.inqVar(sst,2)	**varname time**
[varname,xtype,dimids,natts] = netcdf.inqVar(sst,3)	**varname 'time_bnds'**
[varname,xtype,dimids,natts] = netcdf.inqVar(sst,4)	**varname 'sst'**

In this step, first I made the matrix called "sst" for data output. After I ordered that the matrix would be read only. I inquired NetCDF library about how many variables exist in the whole dataset. What I need are "latitude", "longitude" and "SST" in the dataset, so by the end of this step, I identified that I needed to extract variable 0, 1 and 4 from this dataset.

Step 2. Identyfy the data what you only need in the file

lat = netcdf.getVar(sst,0);	**lat**
lon = netcdf.getVar(sst,1);	**lon**
sstmonth = netcdf.getVar(sst,4);	**sstmonth**

In this step, I asked the MatLab to retrieve the variable 0, 1 and 4 in this dataset.

Step 3. Investigate the file if conversion or/and getting rid of bugs is required

Jan = [];	**Jan**
for i = 1:180	
for j = 1: 89	

```
JAN (i,j) = mean(sstmonth(i,j,1405:12:1753),3);

end

end
```

JAN

The purpose of this step was taking a peek in the dataset because we often have to convert the raw data. For example temperature 20.00 may be input as 2 in the dataset.

Here I made the matrix called "Jan", and I could define longitude and latitude as i = 1:180, j = 1:89 by looking at the matrix made from Step 2. As a test, here I extracted the January data from 1967-1996. Since the matrix 3 dimensional cell 1405 in this dataset means January 1967 and the matrix 3 dimensional cell 1753 means January 1996, I asked MatLab to retrieve the cell from 1405 to 1753 every 12 cells for January collection from 1967-1996.

Step 4. Convert the file into a standard unit (if necessary)

Depending on the result of Step 3, we will have to convert all or some of the data. This step is relatively easy to understand as we can apply the same exact equation which we use Microsoft Excel. After this step, the dataset are ready to be plotted for graphs or maps.

Appendix B. Coral Sr/Ca raw data.

Sample name	Sample number	Sr/Ca (mmol/mol)	Sr/Ca Anomaly (mmol/mol)
GG A1-A 1	1	8.859	0.005
GG A1-A 2	2	8.874	0.019
GG A1-A 3	3	8.914	0.060
GG A1-A 4	4	8.920	0.065
GG A1-A 5	5	8.932	0.078
GG A1-A 6	6	8.885	0.030
GG A1-A 7	7	8.827	-0.028
GG A1-A 8	8	8.816	-0.039
GG A1-A 9	9	8.778	-0.077
GG A1-A 10	10	8.795	-0.060
GG A1-A 11	11	8.809	-0.046
GG A1-A 12	12	8.804	-0.050
GG A1-A 13	13	8.813	-0.041
GG A1-A 14	14	8.885	0.030
GG A1-A 15	15	8.867	0.013
GG A1-A 16	16	8.884	0.029
GG A1-A 17	17	8.874	0.019
GG A1-A 18	18	8.856	0.001
GG A1-A 19	19	8.841	-0.014
GG A1-A 20	20	8.880	0.025
GG A1-A 21	21	8.876	0.021
GG A1-A 22	22	8.844	-0.011
GG A1-A 23	23	8.844	-0.011
GG A1-A 24	24	8.795	-0.060
GG A1-A 25	25	8.788	-0.066
GG A1-A 26	26	8.839	-0.015
GG A1-A 27	27	8.825	-0.029
GG A1-A 28	28	8.806	-0.049
GG A1-A 29	29	8.845	-0.010
GG A1-A 30	30	8.859	0.004
GG A1-A 31	31	8.854	0.000
GG A1-A 32	32	8.858	0.003
GG A1-A 33	33	8.824	-0.031
GG A1-A 34	34	8.774	-0.080
GG A1-A 35	35	8.816	-0.039
GG A1-A 36	36	8.760	-0.094
GG A1-A 37	37	8.781	-0.073

GG A1-A 38	38	8.847	-0.008
GG A1-A 39	39	8.867	0.012
GG A1-A 40	40	8.881	0.026
GG A1-A 41	41	8.922	0.067
GG A1-A 42	42	8.872	0.017
GG A1-A 43	43	8.865	0.010
-	44	-	-0.015
GG A1-A 45	45	8.816	-0.039
GG A1-A 46	46	8.793	-0.062
GG A1-A 47	47	8.786	-0.069
GG A1-A 48	48	8.770	-0.084
GG A1-A 49	49	8.816	-0.039
GG A1-A 50	50	8.863	0.008
GG A1-A 51	51	8.859	0.004
GG A1-A 52	52	8.882	0.027
GG A1-A 53	53	8.891	0.037
GG A1-A 54	54	8.852	-0.003
GG A1-A 55	55	8.839	-0.015
GG A1-A 56	56	8.881	0.026
GG A1-A 57	57	8.852	-0.003
GG A1-A 58	58	8.855	0.001
GG A1-A 59	59	8.856	0.001
GG A1-A 60	60	8.801	-0.054
GG A1-A 61	61	8.823	-0.032
GG A1-A 62	62	8.881	0.026
GG A1-A 63	63	8.899	0.045
GG A1-A 64	64	8.933	0.078
GG A1-A 65	65	8.939	0.085
GG A1-A 66	66	8.913	0.059
GG A1-A 67	67	8.865	0.011
GG A1-A 68	68	8.850	-0.005
GG A1-A 69	69	8.852	-0.003
GG A1-A 70	70	8.820	-0.034
GG A1-A 71	71	8.810	-0.045
GG A1-A 72	72	8.801	-0.054
GG A1-A 73	73	8.810	-0.045
GG A1-A 74	74	8.848	-0.007
GG A1-A 75	75	8.888	0.034
GG A1-A 76	76	8.862	0.007
GG A1-A 77	77	8.871	0.017
GG A1-A 78	78	8.888	0.034

GG A1-A 79	79	8.861	0.007
GG A1-A 80	80	8.877	0.022
GG A1-A 81	81	8.871	0.016
GG A1-A 82	82	8.881	0.026
GG A1-A 83	83	8.887	0.032
GG A1-A 84	84	8.826	-0.028
-	85	-	-0.014
GG A1-A 86	86	8.855	0.000
GG A1-A 87	87	8.816	-0.039
GG A1-A 88	88	8.794	-0.061
GG A1-A 89	89	8.824	-0.030
GG A1-A 90	90	8.871	0.016
GG A1-A 91	91	8.881	0.026
GG A1-A 92	92	8.860	0.005
GG A1-A 93	93	8.883	0.028
GG A1-A 94	94	8.947	0.092
GG A1-A 95	95	8.876	0.022
GG A1-A 96	96	8.756	-0.099
GG A1-A 97	97	8.850	-0.005
GG A1-A 98	98	8.808	-0.047
GG A1-A 99	99	8.786	-0.068
GG A1-A 100	100	8.808	-0.047
10GG A1-A 101	101	8.781	-0.074
10GG A1-A 102	102	8.837	-0.017
10GG A1-A 103	103	8.798	-0.057
10GG A1-A 104	104	8.863	0.008
10GG A1-A 105	105	8.868	0.013
10GG A1-A 106	106	8.869	0.015
10GG A1-A 107	107	8.877	0.022
10GG A1-A 108	108	8.847	-0.008
10GG A1-A 109	109	8.828	-0.026
10GG A1-A 110	110	8.795	-0.059
10GG A1-B 111	111	8.829	-0.026
10GG A1-B 112	112	8.834	-0.021
10GG A1-B 113	113	8.840	-0.015
10GG A1-B 114	114	8.882	0.027
10GG A1-B 115	115	8.984	0.129
10GG A1-B 116	116	8.861	0.007
10GG A1-B 117	117	8.865	0.010
10GG A1-B 118	118	8.886	0.031
10GG A1-B 119	119	8.887	0.033

10GG A1-B 120	120	8.898	0.043
10GG A1-B 121	121	8.888	0.033
10GG A1-B 122	122	8.826	-0.029
10GG A1-B 123	123	8.825	-0.029
10GG A1-B 124	124	8.776	-0.079
10GG A1-B 125	125	8.817	-0.037
10GG A1-B 126	126	8.828	-0.027
10GG A1-B 127	127	8.799	-0.056
10GG A1-B 128	128	8.870	0.015
10GG A1-B 129	129	8.852	-0.003
10GG A1-B 130	130	8.873	0.019
10GG A1-B 131	131	8.889	0.034
10GG A1-B 132	132	8.854	0.000
10GG A1-B 133	133	8.828	-0.027
10GG A1-B 134	134	8.843	-0.011
10GG A1-B 135	135	8.850	-0.005
10GG A1-B 136	136	8.820	-0.035
10GG A1-B 137	137	8.805	-0.050
10GG A1-B 138	138	8.814	-0.041
10GG A1-B 139	139	8.875	0.020
10GG A1-B 140	140	8.885	0.030
10GG A1-B 141	141	8.854	-0.001
10GG A1-B 142	142	8.854	-0.001
10GG A1-B 143	143	8.837	-0.018
10GG A1-B 144	144	8.846	-0.009
10GG A1-B 145	145	8.834	-0.021
10GG A1-B 146	146	8.838	-0.017
10GG A1-B 147	147	8.824	-0.031
10GG A1-B 148	148	8.848	-0.007
10GG A1-B 149	149	8.847	-0.007
10GG A1-B 150	150	8.894	0.039
10GG A1-B 151	151	8.831	-0.024
10GG A1-B 152	152	8.869	0.014
10GG A1-B 153	153	8.910	0.056
10GG A1-B 154	154	8.902	0.047
10GG A1-B 155	155	8.909	0.055
10GG A1-B 156	156	8.871	0.017
10GG A1-B 157	157	8.857	0.003
10GG A1-B 158	158	8.873	0.018
10GG A1-B 159	159	8.841	-0.014
10GG A1-B 160	160	8.814	-0.041

10GG A1-B 161	161	8.764	-0.091
10GG A1-B 162	162	8.782	-0.073
10GG A1-B 163	163	8.771	-0.084
10GG A1-B 164	164	8.817	-0.038
10GG A1-B 165	165	8.836	-0.019
10GG A1-B 166	166	8.846	-0.008
10GG A1-B 167	167	8.875	0.020
10GG A1-B 168	168	8.858	0.003
10GG A1-B 169	169	8.825	-0.030
10GG A1-B 170	170	8.810	-0.045
10GG A1-B 171	171	8.821	-0.034
10GG A1-B 172	172	8.801	-0.054
10GG A1-B 173	173	8.843	-0.011
10GG A1-B 174	174	8.849	-0.005
10GG A1-B 175	175	8.802	-0.052
10GG A1-B 176	176	8.835	-0.020
10GG A1-B 177	177	8.844	-0.011
10GG A1-B 178	178	8.863	0.008
10GG A1-B 179	179	8.900	0.045
10GG A1-B 180	180	8.853	-0.001
10GG A1-B 181	181	8.814	-0.040
10GG A1-B 182	182	8.820	-0.035
10GG A1-B 183	183	8.823	-0.032
10GG A1-B 184	184	8.797	-0.058
10GG A1-B 185	185	8.837	-0.017
10GG A1-B 186	186	8.819	-0.036
10GG A1-B 187	187	8.805	-0.050
10GG A1-B 188	188	8.799	-0.055
10GG A1-B 189	189	8.896	0.042
10GG A1-B 190	190	8.911	0.056
10GG A1-B 191	191	8.926	0.071
10GG A1-B 192	192	8.898	0.043
10GG A1-B 193	193	8.893	0.038
10GG A1-B 194	194	8.891	0.037
10GG A1-B 195	195	8.854	0.000
10GG A1-B 196	196	8.823	-0.031
10GG A1-B 197	197	8.821	-0.034
10GG A1-B 198	198	8.796	-0.059
10GG A1-B 199	199	8.815	-0.040
10GG A1-B 200	200	8.835	-0.020
10GG A-1-b 201	201	8.879	0.025

10GG A-1-b 202	202	8.883	0.029
10GG A-1-b 203	203	8.868	0.014
10GG A-1-b 204	204	8.895	0.041
10GG A-1-b 205	205	8.884	0.030
10GG A-1-b 206	206	8.888	0.033
10GG A-1-b 207	207	8.823	-0.031
10GG A-1-b 208	208	8.856	0.002
10GG A-1-b 209	209	8.844	-0.011
10GG A-1-b 210	210	8.834	-0.021
10GG A-1-b 211	211	8.842	-0.013
10GG A-1-b 212	212	8.877	0.022
10GG A-1-b 213	213	8.897	0.042
10GG A-1-b 214	214	8.926	0.071
10GG A-1-b 215	215	8.938	0.084
10GG A-1-b 216	216	8.974	0.119
10GG A-1-b 217	217	8.963	0.109
10GG A-1-b 218	218	8.858	0.004
10GG A-1-b 219	219	8.850	-0.005
10GG A-1-b 220	220	8.847	-0.008
10GG A-1-b 221	221	8.831	-0.024
10GG A-1-b 222	222	8.817	-0.037
10GG A-1-b 223	223	8.846	-0.009
10GG A-1-b 224	224	8.880	0.026
10GG A-1-b 225	225	8.889	0.034
10GG A-1-b 226	226	8.907	0.052
10GG A-1-b 227	227	8.916	0.061
10GG A-1-b 228	228	8.924	0.069
10GG A-1-b 229	229	8.911	0.056
10GG A-1-b 230	230	8.871	0.016
10GG A-1-b 231	231	8.839	-0.015
10GG A-1-b 232	232	8.803	-0.051
10GG A-1-b 233	233	8.772	-0.082
10GG A-1-b 234	234	8.783	-0.072
10GG A-1-b 235	235	8.788	-0.066
10GG A-1-b 236	236	8.788	-0.066
10GG A-1-b 237	237	8.832	-0.023
10GG A-1-b 238	238	8.850	-0.005
10GG A-1-b 239	239	8.892	0.037
10GG A-1-b 240	240	8.917	0.062
10GG A-1-b 241	241	8.918	0.063
10GG A-1-b 242	242	8.847	-0.008

10GG A-1-b 243	243	8.788	-0.066
10GG A-1-b 244	244	8.853	-0.001
10GG A-1-b 245	245	8.779	-0.075
10GG A-1-b 246	246	8.792	-0.063
10GG A-1-b 247	247	8.802	-0.053
10GG A-1-b 248	248	8.808	-0.047
10GG A-1-b 249	249	8.826	-0.029
10GG A-1-b 250	250	8.856	0.001
10GG A-1-b 251	251	8.882	0.027
10GG A-1-b 252	252	8.922	0.067
10GG A-1-b 253	253	8.892	0.037
10GG A-1-b 254	254	8.840	-0.015
10GG A-1-b 255	255	8.822	-0.033
10GG A-1-b 256	256	8.800	-0.055
10GG A-1-b 257	257	8.808	-0.047
10GG A-1-b 258	258	8.795	-0.060
10GG A-1-b 259	259	8.768	-0.087
10GG A-1-b 260	260	8.856	0.002
10GG A-1-b 261	261	8.831	-0.024
10GG A-1-b 262	262	8.844	-0.010
10GG A-1-b 263	263	8.832	-0.022
10GG A-1-b 264	264	8.837	-0.017
10GG A-1-b 265	265	8.841	-0.014
10GG A-1-b 266	266	8.801	-0.054
10GG A-1-b 267	267	8.784	-0.071
10GG A-1-b 268	268	8.800	-0.054
10GG A-1-b 269	269	8.775	-0.080
10GG A-1-b 270	270	8.788	-0.067
10GG A-1-b 271	271	8.778	-0.077
10GG A-1-b 272	272	8.807	-0.048
10GG A-1-b 273	273	8.857	0.002
10GG A-1-b 274	274	8.866	0.011
10GG A-1-b 275	275	8.891	0.036
10GG A-1-b 276	276	8.904	0.049
10GG A-1-b 277	277	8.873	0.019
10GG A-1-b 278	278	8.828	-0.027
10GG A-1-b 279	279	8.833	-0.022
10GG A-1-b 280	280	8.805	-0.049
10GG A-1-b 281	281	8.815	-0.039
10GG A-1-b 282	282	8.794	-0.060
10GG A-1-b 283	283	8.803	-0.052

10GG A-1-b 284	284	8.826	-0.029
10GG A-1-b 285	285	8.828	-0.027
10GG A-1-b 286	286	8.864	0.010
10GG A-1-b 287	287	8.873	0.018
10GG A-1-b 288	288	8.837	-0.018
10GG A-1-b 289	289	8.809	-0.045
10GG A-1-b 290	290	8.804	-0.051
10GG A-1-b 291	291	8.820	-0.035
10GG A-1-b 292	292	8.742	-0.113
10GG A-1-b 293	293	8.762	-0.093
10GG A-1-b 294	294	8.788	-0.067
10GG A-1-b 295	295	8.812	-0.042
10GG A-1-b 296	296	8.862	0.008
10GG A-1-b 297	297	8.840	-0.015
10GG A-1-b 298	298	8.841	-0.013
10GG A-1-b 299	299	8.831	-0.024
10GG A-1-b 300	300	8.834	-0.021
GG A1-B 301	301	8.838	-0.017
GG A1-B 302	302	8.820	-0.035
GG A1-B 303	303	8.766	-0.089
GG A1-B 304	304	8.813	-0.041
GG A1-B 305	305	8.824	-0.030
GG A1-B 306	306	8.857	0.002
GG A1-B 307	307	8.868	0.014
GG A1-B 308	308	8.856	0.001
GG A1-B 309	309	8.828	-0.027
GG A1-B 310	310	8.777	-0.077
GG A1-B 311	311	8.763	-0.091
GG A1-B 312	312	8.805	-0.050
GG A1-B 313	313	8.789	-0.066
GG A1-B 314	314	8.774	-0.081
GG A1-B 315	315	8.781	-0.074
GG A1-B 316	316	8.835	-0.020
GG A1-B 317	317	8.849	-0.006
GG A1-B 318	318	8.869	0.014
GG A1-B 319	319	8.854	-0.001
GG A1-B 320	320	8.832	-0.023
GG A1-B 321	321	8.837	-0.018
GG A1-B 322	322	8.820	-0.035
GG A1-B 323	323	8.798	-0.057
GG A1-B 324	324	8.797	-0.058

GG A1-B 325	325	8.822	-0.033
GG A1-B 326	326	8.826	-0.029
GG A1-B 327	327	8.862	0.008
GG A1-B 328	328	8.870	0.015
GG A1-B 329	329	8.898	0.044
GG A1-B 330	330	8.885	0.031
GG A1-B 331	331	8.869	0.015
GG A1-B 332	332	8.852	-0.003
GG A1-B 333	333	8.825	-0.029
GG A1-B 334	334	8.801	-0.054
GG A1-B 335	335	8.807	-0.048
GG A1-B 336	336	8.786	-0.069
GG A1-B 337	337	8.842	-0.013
GG A1-B 338	338	8.884	0.029
GG A1-B 339	339	8.868	0.013
GG A1-B 340	340	8.896	0.041
GG A1-B 341	341	8.868	0.013
GG A1-B 342	342	8.874	0.019
GG A1-B 343	343	8.839	-0.015
GG A1-B 344	344	8.843	-0.012
GG A1-B 345	345	8.835	-0.020
GG A1-B 346	346	8.802	-0.053
GG A1-B 347	347	8.794	-0.061
GG A1-B 348	348	8.803	-0.052
GG A1-B 349	349	8.794	-0.061
-	350	-	-0.039
GG A1-B 351	351	8.839	-0.016
GG A1-B 352	352	8.858	0.004
GG A1-B 353	353	8.863	0.008
GG A1-B 354	354	8.889	0.035
GG A1-B 355	355	8.880	0.025
GG A1-B 356	356	8.840	-0.014
GG A1-B 357	357	8.840	-0.015
GG A1-B 358	358	8.819	-0.036
GG A1-B 359	359	8.803	-0.052
GG A1-B 360	360	8.789	-0.066
GG A1-B 361	361	8.789	-0.066
GG A1-B 362	362	8.813	-0.042
GG A1-B 363	363	8.875	0.020
GG A1-B 364	364	8.882	0.028
GG A1-B 365	365	8.910	0.055

GG A1-B 366	366	8.909	0.055
GG A1-B 367	367	8.888	0.033
GG A1-B 368	368	8.868	0.013
GG A1-B 369	369	8.842	-0.012
GG A1-B 370	370	8.814	-0.041
GG A1-B 371	371	8.801	-0.053
GG A1-B 372	372	8.785	-0.069
GG A1-B 373	373	8.804	-0.050
GG A1-B 374	374	8.854	0.000
GG A1-B 375	375	8.879	0.025
GG A1-B 376	376	8.879	0.024
GG A1-B 377	377	8.886	0.031
GG A1-B 378	378	8.909	0.054
GG A1-B 379	379	8.880	0.026
GG A1-B 380	380	8.854	-0.001
GG A1-B 381	381	8.838	-0.017
GG A1-B 382	382	8.812	-0.042
GG A1-B 383	383	8.839	-0.015
GG A1-B 384	384	8.810	-0.044
GG A1-B 385	385	8.803	-0.052
GG A1-B 386	386	8.804	-0.051
GG A1-B 387	387	8.823	-0.032
10GG A1-C 728	388	8.794	-0.061
10GG A1-C 729	389	8.843	-0.011
10GG A1-C 730	390	8.859	0.004
10GG A1-C 731	391	8.849	-0.006
10GG A1-C 732	392	8.912	0.058
10GG A1-C 733	393	8.907	0.053
10GG A1-C 734	394	8.889	0.034
10GG A1-C 735	395	8.851	-0.004
10GG A1-C 736	396	8.831	-0.024
10GG A1-C 737	397	8.833	-0.021
10GG A1-C 738	398	8.827	-0.028
10GG A1-C 739	399	8.823	-0.031
10GG A1-C 740	400	8.822	-0.033
10GG A1-C 741	401	8.860	0.005
10GG A1-C 742	402	8.867	0.012
10GG A1-C 743	403	8.899	0.044
10GG A1-C 744	404	8.887	0.033
10GG A1-C 745	405	8.891	0.036
10GG A1-C 746	406	8.878	0.024

10GG A1-C 747	407	8.864	0.009
10GG A1-C 748	408	8.867	0.013
10GG A1-C 749	409	8.848	-0.007
10GG A1-C 750	410	8.822	-0.032
10GG A1-C 751	411	8.817	-0.037
10GG A1-C 752	412	8.852	-0.003
10GG A1-C 753	413	8.808	-0.047
10GG A1-C 754	414	8.820	-0.035
10GG A1-C 755	415	8.877	0.023
10GG A1-C 756	416	8.899	0.045
10GG A1-C 757	417	8.868	0.013
10GG A1-C 758	418	8.879	0.025
10GG A1-C 759	419	8.890	0.036
10GG A1-C 760	420	8.864	0.009
10GG A1-C 761	421	8.851	-0.004
10GG A1-C 762	422	8.858	0.003
10GG A1-C 763	423	8.835	-0.020
10GG A1-C 764	424	8.795	-0.060
10GG A1-C 765	425	8.805	-0.050
10GG A1-C 766	426	8.842	-0.013
10GG A1-C 767	427	8.797	-0.058
10GG A1-C 768	428	8.902	0.047
10GG A1-C 769	429	8.924	0.069
10GG A1-C 770	430	8.910	0.055
10GG A1-C 771	431	8.852	-0.003
10GG A1-C 772	432	8.838	-0.017
10GG A1-C 773	433	8.830	-0.025
10GG A1-C 774	434	8.831	-0.024
10GG A1-C 775	435	8.817	-0.038
10GG A1-C 776	436	8.830	-0.025
10GG A1-C 777	437	8.843	-0.011
10GG A1-C 778	438	8.853	-0.002
10GG A1-C 779	439	8.918	0.063
10GG A1-C 780	440	8.932	0.077
10GG A1-C 781	441	8.900	0.046
10GG A1-C 782	442	8.874	0.019
10GG A1-C 783	443	8.877	0.022
10GG A1-C 784	444	8.865	0.010
10GG A1-C 785	445	8.880	0.026
10GG A1-C 786	446	8.864	0.009
10GG A1-C 787	447	8.827	-0.027

10GG A1-C 788	448	8.867	0.012
10GG A1-C 789	449	8.755	-0.099
10GG A1-C 790	450	8.910	0.055
10GG A1-C 791	451	8.939	0.085
10GG A1-C 792	452	8.926	0.072
10GG A1-C 793	453	8.927	0.072
10GG A1-C 794	454	8.909	0.054
10GG A1-C 795	455	8.876	0.021
10GG A1-C 796	456	8.870	0.015
10GG A1-C 797	457	8.865	0.011
10GG A1-C 798	458	8.834	-0.020
10GG A1-C 799	459	8.878	0.024
10GG A1-C 800	460	8.923	0.069
10GG A1-C 801	461	8.925	0.070
10GG A1-C 802	462	8.939	0.085
10GG A1-C 803	463	8.953	0.098
10GG A1-C 804	464	8.936	0.081
10GG A1-C 805	465	8.902	0.048
10GG A1-C 806	466	8.866	0.012
10GG A1-C 807	467	8.843	-0.012
10GG A1-C 808	468	8.832	-0.023
10GG A1-C 809	469	8.835	-0.020
10GG A1-C 810	470	8.809	-0.046
10GG A1-C 811	471	8.810	-0.045
10GG A1-C 812	472	8.788	-0.066
10GG A1-C 813	473	8.893	0.038
10GG A1-C 814	474	8.890	0.035
10GG A1-C 815	475	8.890	0.035
10GG A1-C 816	476	8.886	0.031
10GG A1-C 817	477	8.887	0.032
10GG A1-C 818	478	8.868	0.013
10GG A1-C 819	479	8.866	0.011
10GG A1-C 820	480	8.856	0.001
10GG A1-C 821	481	8.848	-0.007
10GG A1-C 822	482	8.846	-0.009
10GG A1-C 823	483	8.906	0.052
10GG A1-C 824	484	8.920	0.066
10GG A1-C 825	485	8.909	0.054
10GG A1-C 826	486	8.915	0.060
10GG A1-C 827	487	8.880	0.025
10GG A1-C 828	488	8.919	0.064

10GG A1-C 829	489	8.864	0.009
10GG A1-C 830	490	8.838	-0.017
10GG A1-C 840	491	8.859	0.005
10GG A1-C 841	492	8.878	0.023
10GG A1-C 842	493	8.913	0.058
10GG A1-C 843	494	8.901	0.046
10GG A1-C 844	495	8.905	0.051
10GG A1-C 845	496	8.883	0.028
10GG A1-C 846	497	8.962	0.107
10GG A1-C 847	498	8.952	0.097
10GG A1-C 848	499	8.975	0.120
10GG A1-C 849	500	8.965	0.111
10GG A1-C 850	501	8.922	0.067
10GG A1-C 851	502	8.916	0.062
10GG A1-C 852	503	8.902	0.048
10GG A1-C 853	504	8.877	0.022
10GG A1-C 854	505	8.852	-0.003
10GG A1-C 855	506	8.859	0.004
10GG A1-C 856	507	8.811	-0.044
10GG A1-C 857	508	8.863	0.008
10GG A1-C 858	509	8.892	0.037
10GG A1-C 859	510	8.893	0.038
10GG A1-C 860	511	8.932	0.077
10GG A1-C 861	512	8.946	0.091
10GG A1-C 862	513	8.948	0.093
10GG A1-C 863	514	8.851	-0.004
10GG A1-C 864	515	8.870	0.016
10GG A1-C 865	516	8.877	0.022
10GG A1-C 866	517	8.910	0.055
10GG A1-C 867	518	8.876	0.021
10GG A1-C 868	519	8.826	-0.029
10GG A1-C 869	520	8.828	-0.026
10GG A1-C 870	521	8.891	0.037
10GG A1-C 871	522	8.903	0.048
10GG A1-C 872	523	8.939	0.084
10GG A1-C 873	524	8.916	0.062
10GG A1-C 874	525	8.921	0.066
10GG A1-C 875	526	8.911	0.056
10GG A1-C 876	527	8.852	-0.003
10GG A1-C 877	528	8.846	-0.008
10GG A1-C 878	529	8.835	-0.020

10GG A1-C 879	530	8.835	-0.019
10GG A1-C 880	531	8.841	-0.014
10GG A1-C 881	532	8.922	0.067
10GG A1-C 882	533	8.943	0.088
10GG A1-C 883	534	8.979	0.124
10GG A1-C 884	535	8.993	0.138
10GG A1-C 885	536	8.973	0.118
10GG A1-C 886	537	8.931	0.076
10GG A1-C 887	538	8.895	0.040
10GG A1-C 888	539	8.865	0.011
10GG A1-C 889	540	8.850	-0.005
10GG A1-C 890	541	8.857	0.002
10GG A1-C 891	542	8.895	0.040
10GG A1-C 892	543	8.893	0.038
10GG A1-C 893	544	8.902	0.047
10GG A1-C 894	545	8.914	0.060
10GG A1-C 895	546	8.922	0.067
10GG A1-C 896	547	8.928	0.073
10GG A1-C 897	548	8.909	0.054
10GG A1-C 898	549	8.870	0.015
10GG A1-C 899	550	8.863	0.008
10GG A1-C 900	551	8.883	0.028
10GG A1-C 901	552	8.840	-0.014
10GG A1-C 902	553	8.844	-0.011
10GG A1-C 903	554	8.787	-0.067
10GG A1-C 904	555	8.860	0.005
10GG A1-C 905	556	8.908	0.053
10GG A1-C 906	557	8.809	-0.046
10GG A1-C 907	558	8.912	0.057
10GG A1-C 908	559	8.883	0.028
10GG A1-C 909	560	8.843	-0.011
10GG A1-C 910	561	8.831	-0.023
10GG A1-C 911	562	8.808	-0.047
10GG A1-C 912	563	8.828	-0.027
10GG A1-C 913	564	8.822	-0.033
10GG A1-C 914	565	8.798	-0.057
10GG A1-C 915	566	8.878	0.023
10GG A1-C 916	567	8.877	0.022
10GG A1-C 917	568	8.895	0.040
10GG A1-C 918	569	8.911	0.057
10GG A1-C 919	570	8.933	0.078

10GG A1-C 920	571	8.926	0.071
10GG A1-C 921	572	8.913	0.058
10GG A1-C 922	573	8.904	0.050
10GG A1-C 923	574	8.868	0.013
10GG A1-C 924	575	8.820	-0.035
10GG A1-C 925	576	8.814	-0.041
10GG A1-C 926	577	8.857	0.002
10GG A1-C 927	578	8.863	0.008
10GG A1-C 928	579	8.885	0.031
10GG A1-C 929	580	8.926	0.072
10GG A1-C 930	581	8.912	0.057
10GG A1-C 931	582	8.929	0.074
10GG A1-C 932	583	8.876	0.022
10GG A1-C 933	584	8.863	0.008
10GG A1-C 934	585	8.863	0.008
10GG A1-C 935	586	8.859	0.004
10GG A1-C 936	587	8.867	0.012
10GG A1-C 937	588	8.822	-0.033
10GG A1-C 938	589	8.854	-0.001
10GG A1-C 939	590	8.866	0.011
10GG A1-C 940	591	8.879	0.024
10GG A1-C 941	592	8.910	0.055
10GG A1-C 942	593	8.918	0.063
10GG A1-C 943	594	8.897	0.043
10GG A1-C 944	595	8.858	0.003
10GG A1-C 945	596	8.870	0.015
10GG A1-C 946	597	8.809	-0.046
10GG A1-C 947	598	8.854	0.000
10GG A1-C 948	599	8.848	-0.007
10GG A1-C 949	600	8.819	-0.036
10GG A1-C 950	601	8.798	-0.057
10GG A1-C 951	602	8.825	-0.029

Appendix C. Public SST dataset raw data.

	Reyn-Smith Olv2	Reyn-Smith Olv1	Noaa Extend SST V3b	Hadley SST
	13.5X144.5 (SSTA) (°C)	13.5X144.5 (SSTA) (°C)	14.0X144.0 (SSTA) (°C)	13.5X14.5 (SSTA) (°C)
Nov-81	0.26	0.31	0.44	0.75
Dec-81	0.32	0.46	-0.10	-0.01
Jan-82	0.64	0.87	-0.63	-0.30
Feb-82	0.48	0.64	-1.05	-0.89
Mar-82	0.34	0.49	-1.06	-1.04
Apr-82	0.09	0.34	-0.70	-0.52
May-82	0.00	0.21	-0.23	0.10
Jun-82	-0.31	-0.19	0.21	0.24
Jul-82	-0.38	-0.25	0.45	0.44
Aug-82	-0.59	-0.47	0.50	0.49
Sep-82	-0.30	-0.16	0.35	0.35
Oct-82	-0.27	-0.17	0.24	0.40
Nov-82	-0.45	-0.39	-0.18	-0.35
Dec-82	-0.54	-0.43	-0.78	-0.77
Jan-83	-0.81	-0.59	-1.58	-1.76
Feb-83	-0.86	-0.69	-1.96	-1.90
Mar-83	-0.63	-0.53	-1.97	-1.98
Apr-83	-0.57	-0.34	-1.47	-1.32
May-83	-0.80	-0.62	-0.87	-0.56
Jun-83	-0.35	-0.21	0.07	0.22
Jul-83	-0.14	-0.03	0.57	0.50
Aug-83	0.20	0.30	0.67	0.87
Sep-83	0.53	0.66	1.28	1.33
Oct-83	0.28	0.44	0.88	0.72
Nov-83	0.33	0.38	0.53	0.50
Dec-83	0.28	0.36	0.10	-0.07
Jan-84	0.36	0.59	-0.59	-0.60
Feb-84	0.39	0.60	-0.88	-0.83
Mar-84	0.48	0.60	-0.80	-0.67
Apr-84	0.56	0.81	-0.29	-0.33
May-84	0.97	1.19	0.42	0.44
Jun-84	0.42	0.51	0.71	0.79
Jul-84	0.69	0.78	0.89	0.97
Aug-84	0.13	0.25	1.08	0.50
Sep-84	0.51	0.59	1.15	0.99

Oct-84	-0.01	0.09	0.67	0.69
Nov-84	-0.02	0.01	0.37	0.31
Dec-84	0.20	0.32	-0.08	-0.29
Jan-85	0.13	0.33	-0.96	-0.84
Feb-85	0.13	0.30	-1.28	-1.04
Mar-85	-0.03	0.11	-1.13	-1.01
Apr-85	0.13	0.38	-0.77	-0.39
May-85	0.20	0.38	-0.14	0.07
Jun-85	0.18	0.33	0.39	0.78
Jul-85	0.14	0.37	0.62	0.87
Aug-85	-0.16	0.00	0.59	0.60
Sep-85	-0.04	-0.01	0.59	0.63
Oct-85	0.00	0.08	0.63	0.45
Nov-85	0.28	0.32	0.53	0.32
Dec-85	0.28	0.41	-0.07	0.14
Jan-86	0.24	0.39	-0.63	-0.63
Feb-86	0.09	0.19	-1.04	-1.10
Mar-86	0.34	0.44	-1.30	-0.98
Apr-86	0.34	0.55	-0.58	-0.51
May-86	0.40	0.60	0.09	0.07
Jun-86	0.20	0.33	0.57	0.55
Jul-86	-0.13	-0.02	0.47	0.58
Aug-86	-0.14	-0.06	0.50	0.54
Sep-86	-0.39	-0.25	0.12	0.33
Oct-86	-0.24	-0.08	0.41	0.58
Nov-86	-0.07	-0.01	0.08	0.35
Dec-86	-0.44	-0.30	-0.72	-0.51
Jan-87	-0.44	-0.23	-1.24	-1.22
Feb-87	-0.22	-0.08	-1.53	-1.50
Mar-87	0.16	0.31	-1.23	-1.12
Apr-87	-0.07	0.18	-0.69	-0.59
May-87	0.09	0.26	0.13	0.00
Jun-87	0.21	0.34	0.38	0.60
Jul-87	-0.12	0.00	0.53	0.66
Aug-87	0.22	0.29	0.79	0.91
Sep-87	-0.20	-0.11	0.70	0.61
Oct-87	0.19	0.26	0.48	0.47
Nov-87	0.29	0.35	0.14	0.15
Dec-87	0.42	0.51	-0.26	0.04
Jan-88	-0.12	0.07	-0.73	-0.87
Feb-88	-0.24	-0.09	-1.17	-1.08

Mar-88	0.16	0.32	-1.10	-0.68
Apr-88	0.28	0.50	-0.51	-0.21
May-88	0.32	0.56	0.06	0.20
Jun-88	0.46	0.52	0.72	0.83
Jul-88	0.47	0.57	0.84	1.06
Aug-88	0.53	0.62	0.92	1.03
Sep-88	0.73	0.81	0.98	1.27
Oct-88	0.60	0.66	0.92	0.96
Nov-88	0.75	0.75	0.48	0.73
Dec-88	0.73	0.78	0.14	0.37
Jan-89	0.67	0.94	-0.31	-0.31
Feb-89	0.70	0.91	-0.59	-0.69
Mar-89	0.84	0.95	-0.77	-0.72
Apr-89	0.74	0.91	-0.23	-0.30
May-89	0.19	0.39	0.16	0.06
Jun-89	0.34	0.43	0.46	0.66
Jul-89	0.43	0.52	0.90	1.08
Aug-89	-0.25	-0.13	0.59	0.90
Sep-89	0.13	0.17	0.76	0.55
Oct-89	-0.08	-0.01	0.56	0.66
Nov-89	0.06	0.10	0.21	0.23
Dec-89	0.23	0.31	-0.53	-0.23
Jan-90	-0.07	0.12	-0.99	-0.76
Feb-90	0.00	0.14	-1.23	-1.09
Mar-90	-0.06	-0.02	-1.28	-1.21
Apr-90	-0.02	0.22	-0.76	-0.84
May-90	0.09	0.36	-0.07	0.01
Jun-90	0.36	0.57	0.47	0.59
Jul-90	0.36	0.49	0.74	0.84
Aug-90	0.49	0.62	0.86	0.97
Sep-90	-0.05	0.11	0.56	0.68
Oct-90	0.09	0.28	0.59	0.65
Nov-90	-0.07	0.09	-0.06	0.05
Dec-90	-0.55	-0.31	-0.64	-0.76
Jan-91	-0.72	-0.28	-1.49	-1.22
Feb-91	-0.58	-0.35	-1.90	-1.59
Mar-91	-0.58	-0.42	-1.89	-1.50
Apr-91	-0.32	-0.09	-0.98	-0.80
May-91	-0.30	-0.15	-0.40	-0.22
Jun-91	-0.22	0.05	0.30	0.33
Jul-91	-0.01	0.27	0.66	0.88

Aug-91	0.38	0.59	0.57	0.92
Sep-91	-0.05	0.10	0.43	0.58
Oct-91	-0.40	-0.21	-0.05	0.15
Nov-91	-0.51	-0.37	-0.34	-0.02
Dec-91	-0.67	-0.55	-0.82	-0.99
Jan-92	-0.33	-0.10	-1.46	-1.52
Feb-92	-0.48	-0.21	-1.60	-1.68
Mar-92	-0.74	-0.52	-1.96	-1.72
Apr-92	-0.71	-0.38	-1.11	-1.17
May-92	-0.65	-0.42	-0.50	-0.56
Jun-92	-0.60	-0.47	0.14	0.07
Jul-92	-0.49	-0.26	0.19	0.46
Aug-92	-0.01	0.11	0.57	0.72
Sep-92	-0.69	-0.55	0.38	0.31
Oct-92	-0.19	-0.04	0.29	0.43
Nov-92	-0.53	-0.42	-0.27	-0.21
Dec-92	-0.80	-0.68	-1.09	-0.67
Jan-93	-1.06	-0.90	-1.76	-1.83
Feb-93	-1.04	-0.90	-1.98	-1.98
Mar-93	-0.71	-0.47	-1.65	-1.86
Apr-93	-0.47	-0.27	-1.12	-1.27
May-93	-0.59	-0.39	-0.57	-0.65
Jun-93	-0.21	-0.06	0.34	0.09
Jul-93	-0.18	-0.18	0.52	0.37
Aug-93	-0.50	-0.35	0.40	0.45
Sep-93	-0.18	-0.04	0.50	0.12
Oct-93	-0.45	-0.28	0.20	0.31
Nov-93	-0.23	-0.12	0.07	-0.19
Dec-93	-0.37	-0.25	-0.73	-0.73
Jan-94	-0.24	0.01	-1.17	-1.01
Feb-94	0.23	0.36	-1.30	-1.05
Mar-94	0.43	0.49	-1.08	-0.71
Apr-94	0.45	0.70	-0.45	-0.30
May-94	0.18	0.31	0.28	0.25
Jun-94	0.39	0.52	0.91	1.10
Jul-94	0.45	0.57	0.75	1.05
Aug-94	0.58	0.64	1.09	1.15
Sep-94	0.53	0.68	1.01	1.38
Oct-94	-0.10	0.12	0.57	0.48
Nov-94	-0.66	-0.57	0.04	-0.15
Dec-94	-0.56	-0.50	-0.68	-0.58

Jan-95	-0.32	-0.11	-1.21	-1.20
Feb-95	-0.55	-0.38	-1.59	-1.41
Mar-95	-0.53	-0.40	-1.67	-1.17
Apr-95	-0.32	-0.09	-0.99	-0.65
May-95	0.14	0.30	-0.23	-0.03
Jun-95	0.12	0.09	0.53	0.67
Jul-95	0.12	0.17	0.77	1.02
Aug-95	0.38	0.48	1.31	1.20
Sep-95	0.46	0.51	1.13	0.98
Oct-95	0.21	0.26	0.97	0.86
Nov-95	0.26	0.32	0.72	0.59
Dec-95	0.44	0.51	0.38	0.25
Jan-96	0.55	0.77	-0.49	-0.46
Feb-96	0.50	0.67	-0.94	-0.80
Mar-96	0.20	0.22	-0.96	-0.67
Apr-96	0.26	0.37	-0.54	-0.17
May-96	0.55	0.70	0.47	0.52
Jun-96	0.47	0.58	0.97	1.00
Jul-96	0.64	0.71	1.09	1.15
Aug-96	0.55	0.57	1.29	0.96
Sep-96	0.44	0.49	1.13	1.07
Oct-96	0.41	0.48	1.15	0.91
Nov-96	-0.09	-0.07	0.49	0.16
Dec-96	0.17	0.18	-0.29	-0.12
Jan-97	0.62	0.81	-0.94	-0.33
Feb-97	0.53	0.69	-1.12	-0.72
Mar-97	0.16	0.24	-1.38	-1.25
Apr-97	0.05	0.41	-0.84	-0.47
May-97	0.30	0.57	-0.07	-0.02
Jun-97	0.53	0.62	0.72	0.65
Jul-97	0.19	0.30	0.95	0.56
Aug-97	0.07	0.31	0.75	0.55
Sep-97	0.09	0.31	0.79	0.85
Oct-97	0.48	0.57	0.96	0.77
Nov-97	-0.41	-0.24	0.40	0.26
Dec-97	-0.35	-0.18	-0.24	-0.35
Jan-98	-0.08	0.12	-1.04	-1.23
Feb-98	0.17	0.33	-1.23	-1.27
Mar-98	0.06	0.19	-1.32	-1.19
Apr-98	0.06	0.30	-0.74	-0.74
May-98	-0.11	0.10	-0.17	-0.22

Jun-98	-0.13	-0.01	0.67	0.33
Jul-98	0.33	0.45	1.05	0.98
Aug-98	0.75	0.86	1.26	1.37
Sep-98	0.72	0.84	1.35	0.96
Oct-98	0.50	0.61	1.06	0.68
Nov-98	0.56	0.62	0.94	0.61
Dec-98	0.49	0.58	0.50	-0.13
Jan-99	0.48	0.69	-0.12	-0.54
Feb-99	0.87	1.04	-0.29	-0.61
Mar-99	0.89	1.03	-0.17	-0.61
Apr-99	0.77	1.00	0.09	-0.37
May-99	0.78	0.98	0.53	0.25
Jun-99	0.54	0.66	0.97	0.75
Jul-99	0.41	0.53	1.17	0.87
Aug-99	0.37	0.49	1.10	0.96
Sep-99	0.52	0.63	1.23	1.21
Oct-99	0.50	0.61	1.15	0.78
Nov-99	0.56	0.61	0.82	0.41
Dec-99	0.33	0.42	0.19	-0.26
Jan-00	0.30	0.50	-0.41	-0.50
Feb-00	0.52	0.68	-0.73	-0.67
Mar-00	0.75	0.88	-0.33	-0.65
Apr-00	0.71	0.93	0.11	-0.35
May-00	0.63	0.83	0.73	0.17
Jun-00	0.51	0.63	1.04	0.75
Jul-00	0.42	0.54	1.13	0.82
Aug-00	0.67	0.81	1.55	1.06
Sep-00	0.31	0.44	1.21	0.78
Oct-00	0.47	0.58	1.03	0.69
Nov-00	0.62	0.65	0.68	0.41
Dec-00	0.34	0.42	0.19	-0.03
Jan-01	0.43	0.63	-0.20	-0.49
Feb-01	0.14	0.29	-0.68	-1.01
Mar-01	0.19	0.31	-0.45	-0.66
Apr-01	0.69	0.91	0.05	-0.22
May-01	0.79	0.89	0.76	0.35
Jun-01	1.11	1.23	1.53	1.42
Jul-01	0.57	0.66	1.28	0.95
Aug-01	0.38	0.47	0.95	0.86
Sep-01	0.63	0.60	0.97	1.20
Oct-01	0.75	0.84	1.16	1.18

Nov-01	0.57	0.63	0.70	0.41
Dec-01	0.29	0.42	0.13	-0.40
Jan-02	0.31	0.51	-0.60	-0.67
Feb-02	0.39	0.55	-0.76	-0.91
Mar-02	0.63	0.76	-0.66	-0.66
Apr-02	0.62	0.86	-0.15	-0.52
May-02	0.57	0.78	0.37	0.04
Jun-02	0.46	0.58	1.07	0.73
Jul-02	0.05	0.16	1.02	0.55
Aug-02	0.14	0.25	1.02	0.74
Sep-02	0.54	0.65	1.09	0.97
Oct-02	0.47	0.57	1.04	0.94
Nov-02	0.44	0.50	0.49	0.69
Dec-02	-0.20	-0.10	-0.17	-0.07
Jan-03	0.08	0.28	-0.68	-0.66
Feb-03	0.02	0.19	-1.09	-1.38
Mar-03	0.13	0.26	-0.84	-1.38

APPENDIX D. Field notes from underwater drilling.

Event	Gabgab Beach (07/26/2010)	Haputo Bay (08/11/2010)
Left Marine Lab	9:15	9:30
Arrived at the dock & launched the boat	9:45	9:45
Arrived at the sample site	10:00	10:30
Deployed the drill & tools underwater	10:30	11:00
Set up the rope around the sample	10:30	11:00
Started drilling	10:30	11:00
Finished drilling	11:00	12:30
Left the sample site	11:30	13:00
Arrived at the dock	11:45	13:45
Arrived at the Marine Lab	12:15	14:15
Washed the drill, tools and hoses	13:00	15:00
Dried and wiped all the tools	13:30	15:30
Sprayed WD-40	13:30	15:30

Field Personnel:
07/26/2010: Jason Miller, Tomoko Bell, Ryan Bell
08/11/2010: Jason Miller, Tomoko Bell, Ryan Bell, John Jenson, Blaz Miklavic

Underwater Drill Technical Support:
Tetsuya Endo
Celery Corporation
1-7-9 Tsumada-Nishi Atsugishi Kanagawa, Japan
Phone: 046-222-0247
E-mail: t-endo@celery.co.jp